Linköping studies in science and technology
Licentiate Thesis Nr. 1956

Evaluation of a melanoma screening framework based on depth resolved light scattering

Motasam Majedy

LINKÖPING UNIVERSITY

LINKÖPING UNIVERSITY

This is an updated version of the thesis

Evaluation of a melanoma screening framework based on depth resolved light scattering

Majedy, Motasam

https://doi.org/10.3384/9789180751155

2023-02-22 The thesis was first published online. The online published version reflects the printed version.

2023-03-07 The thesis was updated with an errata list which is also downloadable from the DOI landing page. Before this date the PDF was downloaded 96 times.

LINKÖPING UNIVERSITY
LINKÖPING UNIVERSITY ELECTRONIC PRESS
https://ep.liu.se

Motasam Majedy
https://doi.org/10.3384/9789180751155

Errata

Page 8, line 16:
The melanin is placed around thus nucleus thus acting as natural sunscreen.
Correction:
The melanin is placed around the nucleus thus acting as natural sunscreen.

Page 9, line 12-14:
This is reflected in the SEER (Surveillance, Epidemiology, and End Results) data where the 5-year survival rate for patents with localized disease, (melanoma that has not spread from the primary site) is approximately.
Correction:
This is reflected in the SEER (Surveillance, Epidemiology, and End Results) data where the 5-year survival rate for patients with localized disease, (melanoma that has not spread from the primary site) is approximately.

Section 1.6.3:
In this thesis, I will discuss the development of the technique utilizing Spatially Modulated Quantitative Spectroscopy (SFDS), which may obviate some of these shortcomings. I will discuss the clinical translation of SFDS, including system optimization.
Correction:
In this thesis, I will discuss the development of the technique utilizing Spatially Modulated Quantitative Spectroscopy (SFDS).

Section 4.2.3, line 12-14:
One example from these phantom measurements is Figure 11, where the blue line shows the reduced scattering coefficient of the dermal phantom alone and the brown line is the reduced scattering coefficient from all the coffee phantoms.

LINKÖPING UNIVERSITY
LINKÖPING UNIVERSITY ELECTRONIC PRESS
Web: https://ep.liu.se E-mail: ep@ep.liu.se

Correction:
One example from these phantom measurements is Figure 11, where the blue line shows the reduced scattering coefficient of the dermal phantom alone and the brown line is the reduced scattering coefficient from the coffee phantom alone.

Figure 12, caption:
The total attenuation coefficient (μt) of white blood cells (WB), red blood cells (LB), and ferrous-stabilized hemoglobin (A0) was measured in both oxygenated (HbO2) and deoxygenated (Hb) samples using the SCT setup.
Correction:
The total attenuation coefficient (μt) of whole blood (WB), lysed blood (LB), and ferrous-stabilized hemoglobin (A0) was measured in both oxygenated (HbO2) and deoxygenated (Hb) samples using the SCT setup.

Figure 14, caption:
The absorption spectra of white blood cells (WB), red blood cells (LB), and ferrous-stabilized hemoglobin (A0) were measured using SFDS on tissue-mimicking phantoms containing Intralipid and hemoglobin.
Correction:
Figure 14 The absorption spectra of whole blood (WB), lysed blood (LB), and ferrous-stabilized hemoglobin (A0) were measured using SFDS on tissue-mimicking phantoms containing Intralipid and hemoglobin.

Linköping studies in science and technology
Licentiate Thesis Nr. 1956

Evaluation of a melanoma screening framework based on depth-resolved light scattering

Licentiate Thesis

Motasam Majedy

Department of Biomedical Engineering
School of Engineering
Linköpings universitet, SE-581 83 Linköping, Sweden
Linköping 2023

This work is licensed under a Creative Commons Attribution 4.0 International License.
https://creativecommons.org/licenses/by/4.0/

Edition 1.0

©Motasam Majedy, 2023

Main supervisor: Rolf Saager, Department of Biomedical Engineering, Linköping University

ISBN 978-91-8075-114-8 (Print)| ISBN 978-91-8075-115-5 (PDF)

ISSN 0280-7971

DOI https://doi.org/10.3384/9789180751155

Cover art: It symbolizes the journey from coffee-fueled chaos to academic enlightenment and the ups and downs of a PhD student's life.

While conducting the research for this thesis, Motasam Majedy was a part of the multidisciplinary doctoral program, Forum Scientium, at Linköping University in Sweden.

Published articles have been reprinted with permission from the respective copyright holder.
Printed by LiU-Tryck, Linköping 2023.

Aknowledgement

Dear readers,

I am honored to present my Licentiate thesis, which represents the culmination of several years of hard work and dedication. This work represents a significant milestone in my academic journey, and I am grateful for the opportunity to contribute to the field of bio-optics.

I would like to extend my heartfelt gratitude to my supervisor Rolf Saager, who has provided invaluable guidance, support, and mentorship throughout this process. Their expertise and encouragement have been instrumental in shaping my understanding of the subject and bringing this work to completion.

Finally, I would like to thank my parents for their unwavering love and support throughout my academic journey. Their encouragement, patience, and understanding have been essential to my success, and I am deeply grateful.

With heartfelt appreciation,

Motasam Majedy

About this book

Melanoma is one of the most aggressive types of skin cancer. When detected at an early-stage treatment is usually successful, however, outcomes are often poor when the disease is detected at an advanced stage. There has been considerable progress in our understanding of the molecular biology, genetics, and immunology of melanoma over the past decade. This has been accompanied by rapid advances in therapeutic strategies for patients with melanoma and an overall improvement in survival rates. However, in spite of these successes, new techniques, and strategies to facilitate early detection, and thus improvements of patient's outcome is needed as mortality remains high. The work in this thesis aims to utilize a novel noninvasive spatial frequency domain spectroscopy (SFDS) based imaging approach to facilitate early detection on melanoma.

Contents

Chapter 1: Introduction – Melanoma and Current Screening and Detection Methods

1.1 Cancer: A disease of uncontrolled cell growth

Cancer is a disease caused by the breakdown in the control mechanism in cells that regulate cell growth and proliferation. There is a growing recognition that cancer represents a major challenge to health care systems, for example, it was anticipated that there were 3.91 million new cases of cancer (excluding non-melanoma skin cancer) and 1.93 million cancer-related deaths in Europe in 2018 [1]. Cancer is often mistakenly viewed as a single entity, however there are over 100 different types of cancer identified, that are classified based on their cellular origin, for example, prostate, breast, colorectal and lung and melanoma are the top five most diagnosed cancers in Sweden today [2]. In addition to differences in cellular origin, cancer can be viewed as two distinct entities, cancer in situ, where the cancer cells proliferate but do not spread beyond the initial site, and metastatic cancer, where the cells proliferate but also acquire the ability to migrate and set up new tumor sites. The latter is responsible for the majority of cancer related deaths since invading tumor cells disrupt normal organ function and are more difficult to treat using conventional therapies. Most cancers begin as localized tumors but can become metastatic due to the accumulation of mutations (changes in the DNA code) in genes that regulate cell growth and survival. Over the past number of years, there has been a gradual shift in cancer treatment, with a push towards more targeted therapies more specific to particular tumor types. At the same time, there has also been pervasive recognition that detection and diagnosis of early stage or pre metastatic tumors can drastically improve survival rates by removing potentially life-threatening lesions before they have the opportunity to spread to distant body sites. New approaches, such as detection of biomarkers or localized/whole body imaging strategies have been utilized to aid in diagnosis. As such new techniques that can be used to identify cancer before it spreads are essential to develop.

1.2 Malignant Melanoma: A cancer of the melanocytes

The majority of this thesis will be focused on a particular type of skin cancer called Melanoma and its early detection strategy using optical methods. To understand melanoma

and how it spreads we must first take a look at the skin. The skin is the largest organ of the body that has many functions, including, protecting the body against trauma and infection, regulation of body temperature, maintaining water and electrolyte balance, sensing stimuli and synthesis of vitamin D. The structure of skin is highly ordered and contains three distinct layers, the epidermis, dermis, and hypodermis. The hypodermis layer is the innermost layer of the skin that contains adipose tissue, lymph, and blood vessels. The dermis that is made up of dense irregular connective tissue, vasculature networks, nerves and supporting cells. The epidermis is the outermost layer and primarily consists of tightly packed stratified epithelial cells. Of the cells present in the epidermis, keratinocytes are most abundant, with smaller populations of melanocytes and Langerhans cells. Keratinocytes that secrete the protein keratin, which provides a protective waterproof coating to the outer layer of the epidermis. The melanocyte also plays a protective role by synthesizing the dark pigment melanin from the amino acid tyrosine. The function of Melanin is to protect the DNA contained within the cell nucleus from damaged induced by UV radiation. Melanocytes secrete melanin into the extracellular environment, which is taken up into neighboring cells. The melanin is placed around thus nucleus thus acting as natural sunscreen. This is evident particularly in fair skinned people where acute UV exposure causes increase melanin production, producing a tan. UV radiation is dangerous for cells. UV can induce oxidative stress by causing damage to protein or lipid complexes in the cells. However, more importantly UV radiation causes DNA damage, primarily by causing crosslinking of the adjacent bases Thymidine (T) that are one of the building blocks of DNA. When DNA damage occurs in genes regulating cell division, this can be catastrophic since mistakes in repairing this damages can lead to cancer development [3].

Malignant melanoma incidence has increased since the early 1970s and numerous studies have shown a correlation between a person's UV exposure, genetic traits, and their risk of developing malignant melanoma [4]. The primary risk factors of developing melanoma are [5]:

- The presence of numerous atypical nevi (moles).
- People with fair skin and blue eyes are more likely to develop malignant melanoma than those with darker skin and brown eyes.
- Malignant melanoma is more likely to develop in people who have high exposure to UV and a history of previous sunburn.

The incidences of melanoma worldwide vary depending on region, but has sharply increased in countries with a higher percentage of fair skinned population over the past decades [6]. The regions with the highest levels are Australia and New Zealand, Europe, and North America. Caucasians with fair skin are more susceptible to developing melanoma, due to lower levels of melanin production and sensitivity to UV induced DNA damage. Behavioral changes in the last decade, such as increased tourism with beginning of low-cost air travel and the use of sun beds may also be responsible for the spike in melanoma rates.

When looking at all incidences of cancer in Sweden, melanoma is the fifth most prevalent cancer type and twelfth most common cause of cancer associated death in both sexes and across all age groups with 4266 and 562 cases respectively in 2020 [7]. The risk of mortality is correlated with detection time, where cases with early detection showing better prognosis compared to those detected at later stages. This is reflected in the SEER (Surveillance, Epidemiology, and End Results) data where the 5-year survival rate for patents with localized disease, (melanoma that has not spread from the primary site) is approximately. 99% compared to patients with distant disease (melanoma that has spread to other body sites) where the 5-year survival rate drops to 30% [8]. These data suggests that treatment of melanoma can be highly effective if found in early stages thus underscoring the critical need for detection and screening techniques.

1.3 How to spot Melanoma: Detection and Staging

Moles, also known as pigmented nevi, are benign growths of melanocytes having the potential to develop into full-blown melanoma. A person usually notices suspect lesions as changes in a pre-existing mole, or the appearance of a new mole. The annual transformation rate of any single mole into melanoma was found to range from 0.0005% in ages under 40s to 0.003% in ages over 60s. According to one study, people with more than 100 moles have a seven-fold higher chance of acquiring melanoma than those with fewer than 15 moles [9]. After consultation with a health care professional, they are usually assigned a dermatologist who will assess their probable lesions using a series of techniques. The first assessment is usually via the naked eye. Most approaches to melanoma diagnosis are based on recognition of evolving lesions, outlier lesions, and particular melanoma characteristics, with the ABCDE

system Figure 1 being the most commonly used to assess the physical properties of a suspect lesion ("A" stands for "Asymmetry," "B" stands for "Border irregularity," "C" stands for "Color variation," "D" stands for "6 mm Diameter," and "E" stands for "evolving lesions") [10]. This step is followed by a dermoscopy and, possibly, a biopsy if the lesion is suspect. In the case of biopsy, a small piece of tissue is excised for histological staining. Although the process works well it is subjective and depends on the presence of skilled dermatologists who have experience in identifying suspect lesions. Furthermore, an accurate diagnosis depends on the clinician's skill. It has been shown that some expertly trained dermatologists have an error rate of less than 80% when diagnosing skin cancer, however they remain a minority among the field [15]. Considering this there have been some suggestions to improve detection using routine screening. A meta-analysis of 15 studies from 2017 found a clinical benefit to skin cancer screening programs [11].

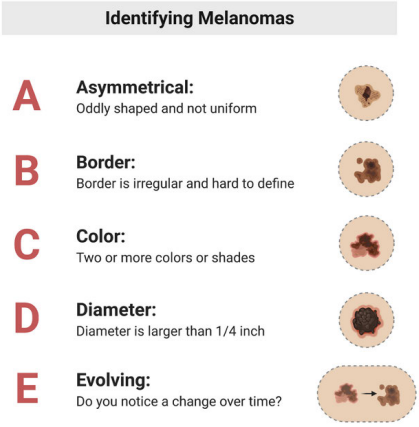

Figure 1 The most popular method for evaluating a suspected lesion's physical characteristics is the ABCDE system.

If a lesion is determined to be suspicious it will have to be confirmed by biopsy and staging. Melanoma was typically staged using two different classification systems to determine how deep the melanoma has invaded into the underlying tissues. To obtain the Breslow Depth, a biopsy is measured with a micrometer in order to determine thickness. Melanomas with a high Breslow depth, >4mm, are considered high grade with an increased risk of metastasis and reduced 5-year survival. Similar to the Breslow Depth, the Clark level uses a staging scale (I-V) to classify how deep the melanoma has invaded the underlying tissues. Like Breslow, tumors with higher Clark stages tend to have a worse prognosis. However, it is worth noting that both Breslow Depth and Clark Level are due to be replaced by the American Joint Committee on Cancer (AJCC) staging system that assigns a stage based on tumor, node,

metastasis (TMN) scores and other prognostic factors [8]. The main message from the Breslow Depth and Clark Levels is that the depth of a melanoma in penetration into the underlying tissue is correlated to patient prognosis and clinical outcome. A major drawback of these staging methods is the need for a tissue biopsy. The process of taking a biopsy and the subsequent histologic interpretation can be time consuming and unpleasant for the patient. Thus, new techniques are needed in order to estimate the level of melanoma invasion (i.e., depth) in a non-invasive manner. A unique biological feature of melanoma is the presence of melanin, making it suited for investigation and detection using bio-optic techniques.

1.4 Tissue oxygenation and hypoxia: connection to skin cancers?

Although the mechanism is complex, low oxygen diffusion in the dermal layer can induce a state of hypoxia and influence the growth rate and aggressiveness of melanoma. The biological mechanisms that cause low oxygenation around the tumor site can be due to disordered or leaky blood vessels resulting in decreased delivery of oxygen from the blood into the tumor core. Alternatively, hypoxia may be caused by an increase in oxygen consumption due to increased metabolic demand of growing tumor cells. Low oxygenation induces a hypoxic response in tissue that is regulated by the activation of specific proteins, called transcription factors, which bind to and activate genes that regulate the cells response to low oxygen. The most well understood is the transcription factor Hypoxia, Inducible Factor 1α (HIF1α). Under normoxic conditions HIF is unstable and is rapidly degraded within the cell. Under conditions of hypoxia, HIF becomes stabilized and locates to the nucleus where it activates a subset of genes that promote survival and angiogenesis, whereby the tumor secretes pro-growth factors that encourage the development of vasculature around the tissue site. It is therefore not surprising that the presence of hypoxia within the body of a tumor is considered an independent marker of a poor prognosis [12]. The presence of hypoxic regions within melanoma has been suggested as a target for therapies. Targeting HIF1α has been shown to reduce tumor growth in a melanoma mouse model [13]. Likewise targeting the process of new blood vessel building (angiogenesis) has also been suggested as a treatment option for melanoma, however the result from clinical trials is mixed and it is not yet apparent if angiogenesis inhibitors will provide clinical benefit for melanoma [14]. Considering the important role that oxygenation plays in melanoma and other solid tumors, novel ways to

assess oxygen availability are needed to improve diagnostics and potentially aid the monitoring of future therapies.

A reoccurring question of this thesis is: can quantitative spectroscopy help clinical practitioners distinguish pigmented lesions by providing information inaccessible to the human eye?

- To detect melanoma early (improved sensitivity)
- To reduce the number of unnecessary biopsies (improved specificity)

To this end, I will summarize some current melanoma screening optical techniques and their limitations and will explain more about the system we have used for our experiments.

1.5 – Current and Emerging Optical Techniques in Melanoma Screening

In this section, I will provide a quick overview of some of the methods of skin cancer screening that utilize using optical techniques to identify potentially malignant lesions. In general, these technologies provide the physician with more information on the lesion to aid in the screening process.

1.5.1 Dermoscope

The dermoscope is primarily used by physicians to aid in clinical screening procedures. The dermoscope is a portable optical instrument with a broadband (white) light source for illumination. It can magnify the field of view, typically by 3–10 times, to provide a doctor with a more accurate representation of the "ABCDE" characteristics of a suspect lesion.

In order to reduce specular reflection and improve visualization of the lesion and its surrounding area, the dermoscope is sometimes used in conjunction with an oil-based substance at the skin's contact surface or cross polarizers [15].

Dermoscopy is frequently used, but it is still a subjective technique that heavily depends on the doctor's skill and perception.

1.5.2 MelaFind

MelaFind is an FDA-approved optical scanner with a software-driven imaging and data analysis tool created to assist a dermatologist in deciding whether to perform a biopsy on a mole that is irregular and pigmented [16]. MelaFind is a multispectral digital dermoscope that captures images of suspected lesions in multiple spectral bands for further computational analysis. It illuminates the lesion with 10 distinct wavelengths from 430nm to 950nm, unlike the typical dermoscope which only uses broadband light.

Imaging data ranging from visible to near infrared wavelengths has the potential to disclose aspects of lesions that are not visible to the human eye. The first step in the image analysis process is segmentation, which identifies the lesion's location and separates it from the surrounding healthy skin. Then, depending on the traits and qualities listed in the "ABCDE" technique, a proprietary algorithm is used to mathematically analyze the 10 images taken at different wavelengths [17].

The lesions characteristics such as granularity, non-uniformity, texture, and morphology are extracted from each image. The sum of all assessed features results in a value that is used by a lesion classifier, which serves as a threshold to distinguish melanoma from nevi, and to categorize the lesion into a specific category. This technique enables regulated and impartial analysis of suspected lesions using automated algorithms. Additional details about the lesion, including texture and structural indicators, such as collagen concentration, beneath the skin's surface, are revealed using near infrared light.

When employing MelaFind, Elbaum et al. found that the diagnosis sensitivity was 81%, which is higher than the sensitivity of conventional dermoscope screening techniques, which is around 50% [17]. While these initial, small population results showed great promise of this multi-spectral image analysis approach, when larger studies were conducted to seek FDA approval, the specificity of MelaFind was reduced to 10%. This was sufficient to gain approval as an adjunct device to standard clinical screening as it had demonstrated a marginal improvement in specificity over that of general clinical screening practitioners.

1.5.3 SIAscope

The SIAscope, or Spectrophotometric Intracutaneous Analysis, is an optical instrument that, makes use of a light source that spans the visible to the near infrared regime (SIA). In addition to visible wavelengths, near infrared light can be used to access the skin's deeper structural elements, such as the collagen matrix. At spatial resolutions of 40 μm or 20 μm per pixel, respectively, images of the skin can be captured over areas of 24 × 24 mm or 12 x 12 mm using SIAscope [18]. A portable device that is connected to a laptop is used to take pictures. To compute the parametric maps, several spectrally filtered images in the 400 nm to 1000 nm range are acquired, calibrated, and processed utilizing proprietary image analysis algorithms. These are then shown on the screen in the form of SIAgraphs with a color image of a lesion [18]. Cotton et al suggested that these image processed results could be qualitatively related to a lesion's thickness (Breslow thickness) of melanoma [19].

In order to determine whether a pigmented legion is malignant, this information is combined with image analysis findings from the SIAscope, such as blood displacement, collagen disruption, and the presence of melanin in the dermis. According to reports, the SIAscope's sensitivity and specificity for detecting melanoma are respectively 80.1 percent and 82.7 percent [20]. However, similar to findings presented for MelaFind, these results only reflect a small population study.

1.5.4 Alternative Clinical Assessment Approaches Utilizing Spectral Imaging

Other spectral imaging approaches applied to clinical research [21] have proposed an alternative strategy for separating cancerous from non-cancerous lesions utilizing a derived correlation factor. In this study the illumination of the mole was done with broadband halogen lamps. Images were detected using a camera and a color filter at intervals of 10 nm between 450nm and 950nm. The wavelength-dependent optical density value was produced by recording the reflected intensities from each wavelength band and comparing them to a baseline reference intensity.

An arbitrary parameter was created for distinguishing lesion malignancy by employing three optical density values at 540nm, 650nm, and 950nm. However, these techniques still lack

specificity when it comes to obtaining functional information, even though these screening tools have the potential to help doctors by simple improvements in biopsy accuracy. Both MelaFind and SIAscope use near-infrared images of lesions to find out their physiology through structural or color shift information, but neither one appears to be able to quantify the amount of chromophores present.

1.5.5 SkinSpect (Spectral Molecular Imaging)

SkinSpect, is a hyperspectral imaging system that consists of spectrally programmable linearly polarized light source that illuminates the skin under investigation at 33 wavelengths evenly spread between 468 nm and 857 nm. For each wavelength, diffusely reflected photons are divided into collinear and cross-polarized image trajectories, and images are then taken [22]. This approach combines polarization and hyperspectral imaging, two depth-sensitive techniques, to precisely map the distribution of hemoglobin oxygenation and melanin in a lesion.

The ability to probe skin in terms of absorption coefficient (μ_a) and reduced scattering coefficient (μ_s'), as well as quantitative functional properties, oxy- and deoxy-hemoglobin concentration, tissue oxygen saturation, and total hemoglobin concentration, is provided by other optical techniques that will be discussed in next section.

1.5.6 Aura (Verisante)

Raman spectroscopy, an optical technique used by Verisante Aura, links the molecular makeup of the cells making up the area being investigated with the spectrum of inelastic scattering of laser light within the skin, which is caused by variations in the molecular vibration of tissue biomolecules. A statistical analysis of the resulting light spectrum supports the skin cancer diagnosis. While this approach claims greater molecular sensitivity than most multispectral imaging techniques, only small population studies have been offered to support this claim and the technology has yet to gain FDA approval.

1.6 Quantitative Optical Techniques for determining physiologic properties of the Skin

Optical Imaging has had a growing impact on the domains of medicine and biology over the past ten years.

Standard laboratory research to understand more about the basic biological processes and validation for better clinical study outcomes are both critical contributions to the field. This success is because of photons' exceptional ability to noninvasively investigate the functional and structural contrast of living tissues at various imaging scales. Numerous optical instruments have been created to quantify these contrast processes on spatial scales ranging from the microscopic (1 um) to the macroscopic (>1 cm) due to variety of the optical source of contrast. The use of these tools by researchers to meet unmet clinical needs has in turn produced some fascinating new findings (Figure 2, taken from [23]). One of the practical problems for using optical methods in many clinical contexts is physicians' need to survey a vast area (>cm) with acceptable resolution (1 mm) in a short period of time (seconds to minutes), all while leveraging endogenous contrast that predicts functional state.

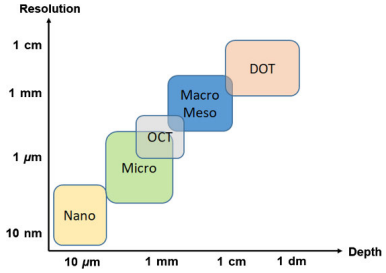

Figure 2 In biomedical optics, there is a trade-off between the depth of imaging and the resolution. SFDI is well-suited for imaging on a larger scale, with a resolution limited by the diffusion of light in tissue and a depth of penetration of up to one centimeter. Other techniques, such as nano and microscopy, OCT, mesoscopy, macroscopy, and DOT, also exist. (Source: Gioux, et.al. [23]).

To describe tissue according to the concentration of physiological chromophores, several optical approaches have been developed for evaluating functional information of the skin. We will briefly touch upon some of these techniques in this section.

1.6.1 Diffuse Optical Spectroscopy

Diffuse Optical Spectroscopy (DOS) is a method for measuring optical characteristics in the near infrared region from 650nm to 1000 nm. This technique employs both frequency modulated lasers and wideband light [13]. The method employed by DOS is a contact probe approach to target illumination and signal detection. Before the light reaches the skin surface, the incident light is frequency modulated in MHz and GHz range. During this process the phase and the amplitude of the incident light changes when the light reaches the skin and interacts with the light-absorbing chromophores and cellular components. The diffusion approximation can be used to extract the absorption and reduced scattering coefficient values at each wavelength. DOS has been widely used in breast cancer and muscle studies due to its deep light penetration depth in the near infrared range.
Tseng et al [24] demonstrate how DOS can be set up to collect data from a more superficial depth (1-2 mm) such as the skin by adjusting for a smaller source-detector separation about 1cm.

1.6.2 Spatial Frequency Domain Imaging

Spatial frequency domain imaging (SFDI), as a mesoscopic and macroscopic technique that meets these broad requirements and contextualizes recent achievements in terms of technological improvements, implementation, and clinical applications. Spectral imaging methods like SFDI can be used to assess absorption and reduced scattering coefficient values together with chromophores concentration maps in addition to non-imaging "point" spectroscopy techniques like DOS.

Although it analyzes wavelength absorption and scattering in a different way, (by projecting of modulated spatial frequencies), it shares many of the fundamental theories used to describe DOS. In SFDI, the AC and DC components of the raw reflectance are extracted from each collected image at a given spatial frequency using a three-phase demodulation algorithm after employing each frequency shifted at three phases. Changes in the instrument response are adjusted for in calibrated AC reflectance of tissue by using a reference phantom with well-known optical characteristics. In order to find specific pairs of values for reduced scattering

coefficient and absorption coefficient that matches the reflectance, a Monte Carlo simulation can be applied.

Both depth and quantitative optical qualities can be derived from the spatial modulation transfer function for the diffusion of light into the tissue for a variety of practical applications, such as melanoma detection. However, because of the comparatively small numbers of lesions evaluated, these studies have considered exploratory and preliminary. Furthermore, the SFDI equipment utilized to make these observations operates in the 650-1050 nm range.

1.6.3 Spatial Frequency Domain Spectroscopy (SFDS)

In this thesis, I will discuss the development of the technique utilizing Spatially Modulated Quantitative Spectroscopy (SFDS), which may obviate some of these shortcomings. I will discuss the clinical translation of SFDS, including system optimization.

SFDS is a quantitative spectroscopy approach that makes use of spatial frequency domain method to obtain absolute optical parameters from a single area over a wide spectral range [25]. Contrary to SFDI, this technique is a high spectral resolution instrument that detects light from a small spot size of 1-2 mm. Furthermore, SFDS can operate in the visible wavelength range as well as the 650-1050nm range typically used by DOS. The double peak, or the alpha and beta bands (530 nm and 575 nm), of oxyhemoglobin, which are often unreachable using traditional SFDI or DOS, can be found by probing into the visible wavelength regime.

It is expected that the distinctive characteristics of the oxy-hemoglobin extinction coefficient associated with these two bands improve the ability to separate melanin from the other tissue chromophores in comparison to techniques that are restricted to operation in the 650nm-1050nm range because the absorption spectrum of melanin is relatively featureless. As a result, SFDS can measure chromophore concentrations more precisely than techniques that are restricted to the 650nm–1050nm wavelength range. This may be helpful in terms of characterization of pigmented tissue, especially lesions that may be clinically worrisome. A further distinctive feature of SFDS is its wide wavelength range that enables access to various depths depending on wavelength dependent light penetration.

The light in the visible range results in a shallower level of interrogation depth because tissue in the visible (430 - 650 nm) range has up to three times more scattering and ten times higher absorption than that in the near infrared (650-1050 nm).

This makes it possible for SFDS to employ depth-resolved spectroscopy of the dermis and epidermis of the skin by utilizing a two-layer heterogeneous skin model, which is more accurate than the more conventional homogeneous chromophore fit.

1.7 Thesis Aims and Objectives

This licentiate thesis details the first half of a PhD project on the development of a new, spectral imaging approach to quantitatively characterize suspected Melanoma lesions. The ultimate goal of this project is to present a non-invasive imaging approach capable of differentiating the optical properties of the lesion from those derived from the underlying tissue. This successful validation of this approach will provide estimates of lesion depth, similar to those reported as Breslow Depths or Clark Scales without the need of biopsies, as well as volume specific spectral analyses of melanin distribution, concentration, structure and microvascular blood concentration and oxygenation immediately beneath it. Depth specific scattering properties may also provide new opportunities to identify cancerous tissue based on its relation to cellular morphology and extra-cellular structures (e.g., collagen formation).

In this licentiate thesis, a spectral depth sensitive model will be proposed that will exploit previously observed differences in scattering properties from melanized tissue over those observed from underlying dermal tissue.

- Chapter 2 will introduce SFDS in greater detail and how previous layer model approaches have exploited this measurement technique to estimate melanin concentrations and distributions, but also describe how the range of tissue depths a two-layer model can be extended over millimeters through using layer specific scattering differences as the source of tissue contrast.
- Chapter 3 will introduce a new approach to describe the depth sensitivity and distribution of interaction of light measured under SFDS across all wavelengths detected, independently. This model of spectral depth sensitivity will include its dependence on the absorption and scattering properties of tissue, but also the impact of

optical aberrations as a function of depth that will impact the interpretation of SFDS data.

- Chapter 4 will focus on the development of traceable standards and measurement methods that will be used to independently validate the accuracy of the proposed two-layer model in the context of (1) determining the thickness of the melanized tissue, as well as (2) the subsequent extraction and interpretation of the layer-specific optical properties. This includes the development of two types of tissue simulating phantoms designed to mimic multiple thickness of pigmented nevi and as well as fully characterized hemoglobin phantoms to assess the spectral integrity of the extracted underlying tissue spectra such that the accuracy can be interpreted in terms of blood concentration and oxygenation.
- Chapter 5 will include a review of publications that resulted from this thesis work.
- Chapter 6 will discuss this progress achieved in this effort to date and how this will fit in the future work towards the completion of this project in the form of a Doctoral Thesis.

Chapter 2: Spatial Modulated Quantitative Spectroscopy (SFDS) and Two-Layer Models of Skin

2.1 – Introduction

The fundamentals of spatial frequency domain imaging (SFDI), which have been extensively discussed by Cuccia et al [26], serve as the foundation for SFDS. I will go over the basics of SFDI in this chapter and the details of SFDS in relation to SFDI will be discussed. The final topic will be the two-layer modeling approach developed from SFDS which in turn allows for layer-specific quantitation of chromophore concentration.

2.2 - Principles of SFDI: A Review

Spatial frequency domain imaging (SFDI) has grown extremely rapidly over the past ten years. This is due in part to its special ability to image optical properties and chromophores rapidly and efficiently over a wide field of view. SFDI's key hardware features will be discussed in this section. A Schematic picture of the SFDS system we use in this thesis is shown in Figure 3. The spectrometer is replaced by a camera in case of SFDI.

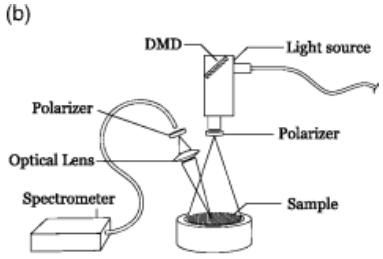

Figure 3 schematic drawing of setup used for SFDS. DMD, digital micromirror device. (Source: Majedy, M., et al. [33]).

2.2.1 Spatially Modulated Illumination

The basis for target illumination in SFDI is a projection of an encoded sinusoidal spatial frequency pattern that alternates between dark and light bands. To project structured light

patterns this instrument employs a broadband halogen lamp or as in some applications, laser diodes or light emitting diodes (LEDs) [23, 27].

By projecting light from the light source through a spatial light modulator (SLM), spatial modulation of illumination can be achieved. Any device such as liquid crystal on silicon (LCos), digital micro-mirror (DMD) or transmission gating that allows for encoding light in two dimensions can be categorized as an SLM. The type of SLM normally used in SFDI that transforms the light delivered from the source into predetermined set patterns of light is shown in Figure 3.

Typically, each SFDI measurement requires the projection of a variety of spatial frequencies onto three phase-shifted images. That is to say, the same spatial frequency is projected three times, each time with an image shifted by an angle of 0, 120, and 240 degrees.

High frequencies, around $0.2mm^{-1}$, are sensitive to reduced scattering, while low spatial frequencies, starting at $0mm^{-1}$, are most sensitive to differences in absorption [26]. So, each SFDI assessment typically employs a broad spectrum of spatial frequencies, ranging from a planar illumination (0th frequency) to $0.2mm^{-1}$. The AC and DC components of the measured light reflectance are separated using the phase-shifted pictures that were obtained at each frequency. Demodulation and data processing will be discussed in greater detail in the post-acquisition processing section.

2.2.2 Camera Based Detection

Light from the SLM is projected onto the tissue, where it interacts with the tissue to produce intensity patterns, which are subsequently captured as a two-dimensional image by a camera.

Cross-polarizing the camera with the light source reduces the amount of specular reflection from the sample's top surface. To further reduce specular reflection the camera could be placed away from the angle of reflectance. Furthermore, a liquid crystal tunable filter utilized together with the camera (here a CCD camera) enables detection wavelength selection while employing a broadband light source. Data is gathered from detected reflectance pictures.

2.2.3 Data Processing

The intensity modulated reflectance is decoupled from the AC and DC amplitudes using the three phase-shifted patterns for each spatial frequency. A look up table is generated using a

forward diffusion model [28, 29] to relate reflectance to reduced scattering coefficient and absorption coefficient as a function of frequency [26]. Due to the two-dimensional nature of the data from the CCD camera data, this lookup table approach is used to determine the demodulated reflectance of every single pixel in the image. To help demonstrate the values for each pixel's absorption and reduced scattering coefficient for a particular wavelength, optical property maps of the image are ultimately constructed with a color scale.

2.3 - Principles of SFDS

For the purposes of comparison with conventional SFDI, I will go over the basics of SFDS in this section. That also includes information on each individual component used in our SFDS instrument.

2.3.1 Spatially Modulated Illumination

A 100-watt, broad-spectrum light source (Quartz Tungsten Halogen) is used for illumination in the SFDS system that we have developed. A fiber bundle delivers the lamp's output to a DMD projector (Agile, CA), where software-controlled sinusoidal intensity patterns are generated and projected to an image plane with at 40x30cm field of view. At least two spatial frequencies at equal step size of 0.05mm-1 and three phase-shifted images for each spatial frequency at 0, 120, and 240 degrees are commonly used in SFDS data gathering. For our experiments we have used 5 different spatial frequencies with equal step size of 0.05 mm-1 ranging from 0 mm-1 to 0.2 mm-1.

2.3.2 Spectrometer based Detection

In SFDS, light reflectance is measured from a central location within the projected illumination pattern on the sample, as opposed to the use of a CCD camera to detect reflectance across the entire field of view in standard SFDI.
In the SFDS system used in these experiments, this small spot has a diameter of 1 mm at the surface of the sample under investigation (e.g., tissue) and is collected by the distal end of the

optical fiber via simple lens. This optical fiber then delivers this light to a spectrometer (Avantes). With this setup, SFDS can measure the optical properties over a wide range of wavelengths in a broad spectrum. The SFDS system that we use in our experiments measures the optical properties ranging from 450 nm to 1050 nm in a single exposure [30-33].

SFDS may not be as precise or cover as large of an area as SFDI, but SFDI is usually limited in that it can only measure the optical properties at a select number of specific wavelengths determined by the LEDs used or filters in front of the camera.
In the visible and near-infrared range, an SFDS system can achieve a 1 nm spectral resolution for absorption and reduced scattering coefficient. To that end, SFDS is typically used in investigational studies where all sources of optical contrast, chromophores in particular, are not known as well as investigations of new light models and complex tissue structures.

2.3.3 SFDS Data Processing

In order to decouple the corresponding AC and DC components of the reflected light, each spatial frequency pattern contains three independent phase-shifted patterns at 0, 120 and 240. that is same as SFDI. These patterns are visualized in Figure 4.
Demodulating the measured reflectance requires at least three phase-shifted images for each spatial frequency, even though theoretically there is no restriction on how many frequencies can be measured or on the increment between them.

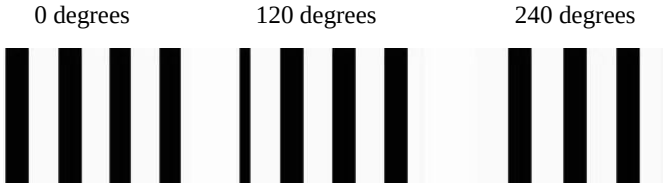

Figure 4 Images of sinusoidal projections that have been shifted in phase, at angles of 0, 120, and 240 degrees in the field of view.

The method for extracting the AC spectrum (M_{ac}) from the total raw reflectance signal is represented by the equation below where I indicate the spectral intensities of each phase-shifted image.

$$M_{AC}(\lambda, f_x) = \frac{\sqrt{2}}{3}\{[I_1(\lambda, f_x) - I_2(\lambda, f_x)]^2 + [I_2(\lambda, f_x) - I_3(\lambda, f_x)]^2 + [I_3(\lambda, f_x) - I_1(\lambda, f_x)]^2\}^{1/2} \quad (1)$$

A reference phantom with known optical properties is used for calibration of the information acquired from the AC component of the measured reflectance. The purpose of this calibration phase is to eliminate any extra light reflectance signal that does not come from the sample itself.

Individual absorption and scattering pairs are generated for each of the 1024 pixels of information using Monte Carlo simulation in conjunction with this effective MTF [25]. Since the diffusion approximation fails in the visible wavelength region, Monte Carlo is utilized as a forward model instead.

The hemoglobin alpha and beta bands in the visible range of wavelengths (530 nm and 575 nm), as well as water and lipid peaks in the near infrared (975 nm and 920 nm) can all be distinguished through 1 nm spectral resolution of SFDS.

With a 1-nm resolution, many of these spectral characteristics will be well-resolved because they span only 20-30nm.

2.4 – Two Layer Models using SFDS

Using the previous models and other studies, [34-36], we see that the measurements we get from SFDS are on a "per volume interrogated" basis, where each wavelength of optical properties from tissue would result from a slightly different volume of tissue. Consequently, if you shine light through a two-layer medium, such as a pigmented nevi, there is an ambiguity as to whether there may be the thicker volume from the nevi being interrogated or a higher concentration of melanin. In the case of melanoma, if the penetration depth is inversely proportional to the amount of absorption and scattering at each wavelength, pure spectral components become distorted as a function of an interrogation volume change, thus it could indicate that the melanoma is chemically altered, or it has gone deeper into the tissue and the distortion is a depth specific artifact. Thus, the detected concentrations and the spectral shape of the detected melanin can be confounded by layer thicknesses.

2.4.1 Absorption-Based Two Layer Model

The depth-resolved optical property quantitation-based model provided by Saager et al [37] assumes a two-layer medium, with the upper layer representing the epidermis, which is composed only of melanin, and the bottom layer representing the dermis and subcutaneous layer, which contain oxy and deoxy-hemoglobin, lipid, and water. SFDS employs broad-spectrum light in the visible and near-infrared ranges, and because light penetration is wavelength-dependent, various levels of penetration are possible. Near-infrared light penetrates deeper into tissue (30 mm) than light in the visible range, which has a surface penetration depth of roughly 150 microns [37]. The amount of light absorbed and scattered by each layer of the skin is relatively proportional to the overall volume of the skin that is being investigated. This is often referred to as the partial volume effect.

The total measured absorption as a function of layer specific absorption is shown in the equation 2, where c represents concentration and l is the distance that light travels, and the epidermis and dermis/subcutaneous layer are denoted by the subscripts 1 and 2, respectively.

$$\mu_{a\,meas}(\lambda) l_{meas}(\lambda) = c_1 \mu_{a1}(\lambda) l_1 + c_2 \mu_{a2}(\lambda) l_2(\lambda) \qquad (2)$$

The two-layer model where the d_1 is the top layer and d_2 is the bottom layer together with the assumed path of the light through both layers is shown in Figure 5.

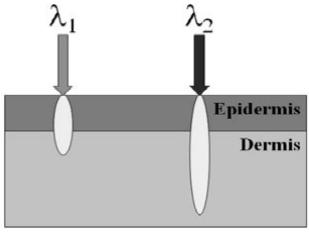

Figure 5 The two-layer model illustrating the epidermis and dermis of skin in which the broadband light probes these layers with concentration of c1 and c2 respectively. (Source: Saager, et.al.[38])

Given that the thickness of the epidermis is similar by all the wavelengths used to perform the measurement, it is expected that light ranging from the visible to near infrared penetrates through the epidermis, keeping the light penetration path of l_1 constant.

The wavelengths of the light being employed, as well as the optical characteristics of the turbid media, or skin, itself, have a significant impact on the path of l_2. The relationship between l_{meas}, l_1, and l_2 may be seen in equation 3 where l_2 is the penetration depth into the dermis which varies depending on the wavelength of the light utilized and the epidermal thickness is represented with l_1.

$$l_{meas}(\lambda) = l_1 + l_2(\lambda) \tag{3}$$

Since it is assumed that the first layer's only absorption source is melanin, the equation (4) can be used to relate the epidermis' thickness and melanin concentration. By applying straightforward least squares fit exclusively for melanin without considering the partial volume effect c_{1meas} can be extracted with SFDS.

$$c_1 = c_{1\,meas}(\lambda)\left(\frac{l_{meas}(\lambda)}{l_1}\right) \tag{4}$$

Similar to layer 1, layer 2 can be approximated by the equation (5) for total concentration and path length. Using SFDS and a least square fit function, it is possible to estimate C_{2meas} as well. So, the epidermal thickness is given as shown in equation (6).

$$c_2 = c_{2\,meas}(\lambda)\left(\frac{l_{meas}(\lambda)}{l_2(\lambda)}\right) = c_{2\,meas}(\lambda)\left(\frac{l_{meas}(\lambda)}{l_{meas}(\lambda) - l_1}\right) \tag{5}$$

$$l_1 = \frac{(c_{2\,meas}(\lambda_1) - c_{2\,meas}(\lambda_2))l_{meas}(\lambda_1)l_{meas}(\lambda_2)}{(c_{2\,meas}(\lambda_1)l_{meas}(\lambda_1) - c_{2\,meas}(\lambda_2)l_{meas}(\lambda_2))} \tag{6}$$

In order to optically eliminate the epidermis in terms of its impact on the overall absorption spectrum, l_1 is derived from equation (6) above and utilized to determine the layer-specific concentration of melanin, c1 from equation (4). Without the presence of melanin, the dermis can be regarded to be homogeneous in terms of chromophores in the skin. The remaining chromophores of relevance can be quantified with greater accuracy using least squares fitting.

2.4.2 Scattering-Based Two Layer Model

This absorption-based approach has exploited these spectral changes in tissue penetration depths to estimate the distribution thickness of melanin and the melanin concentration in different healthy skin types and superficial moles up to 100-200 micron in depth [38]. Staging of melanoma, however, requires a technique for depths of 1-4 mm. Therefore, the scattering-based technique used in this project is uniquely suited to facilitate melanoma staging. To probe the layer thickness deeper than what has been done before (100-200 µm) we need a two-layer model and source of optical contrast that can extend as deep as the melanin goes. The hypothesis is that the melanin absorption will significantly impact the light penetration as a function of wavelength. Since melanin is highly absorbing in the visible range, the penetration depth becomes incrementally more superficial when encountering a heavily melanized tissue, yet penetration depths can still reach millimeters in the near infrared.

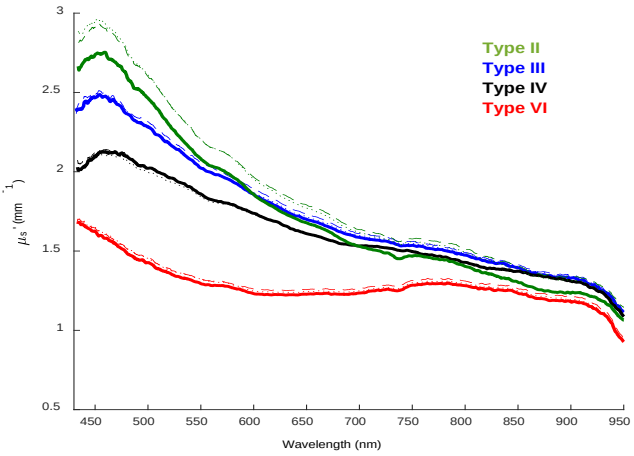

Figure 6 Measured scattering spectra from four representative skin types on the Fitzpatrick scale [39]. Observed from these spectra is that the scattering in the visible regime decreases as epidermal melanin increases and in the case of dark skin pigmentation (skin type VI), the measured scattering spectrum no longer follows a simple power law as expected in homogenous tissue scattering. (Source: Saager, et.al. [39])

In a previous study, the reduced scattering coefficient spectra derived from four skin types (Fitzpatrick skin types II, III, IV, and VI) using SFDS measurements (Figure 6) showed that, the instead of scattering following a power law like what one could see in a single layer, it began to reduce in size and get more complicated in darker skin (skin type VI)[39]. This suggests that scattering for melanoma as in for darker skin type used in this study, may not fit to a single power law and is more complex. However, we can utilize the depth penetration estimate and have two separate scattering, one for the melanized tissue and one underlying

tissue scattering properties. Moreover, we can map out and see where the transition between one scattering properties and the other is and use that as a meter stick for the scattering as a means to estimate layer thickness. On the other hand, this helps to probe a range from 200 micron all the way down to around 3 mm into the tissue and therefore have a better depth estimation of melanoma. So, using a layered model, SFDS would provide quantitative functional information on the layer-specific chromophores present in tissue.

In its formulation, the scattering-based model shares a considerable amount of similarities with its absorption counterpart as they both presume two layers, the penetration depths of the optical measurements vary as a function of wavelengths, and that due to the partial volume effect, the measured scattering spectrum will have varying contributions from the layers. The key distinction, however, is that given the relatively featureless nature of the scattering spectra, the two-layer model is no longer constrained to levering discrete regions in the visible to the near infrared. In the scattering case, the transition between contributions between layers can now be treated continuously across the visible and near infrared, allowing for layer thickness estimates to extend to depths of millimeters as contributions from the bottom layer need only to be detected in the NIR and not the visible. To that end, we propose an initial model to describe the measured reduced scattering spectrum as follows:

$$\mu'_{s_{meas}}(\lambda) = \alpha(\lambda)\mu'_{s_1}(\lambda) + (1 - \alpha(\lambda))\mu'_{s_2}(\lambda) \qquad (7)$$

Here $\mu'_{s_1}(\lambda)$ represents the scattering spectrum from the top layer, $\mu'_{s_2}(\lambda)$ from the bottom layer and $\alpha(\lambda)$ represents the relative contribution from the top in a partial volume sense. In this context $\alpha(\lambda)$ is a unitless parameter that is bounded between 0 and 1. The analog of this parameter in the absorption model is the ratio of $l_1/l_{meas}(\lambda)$, how it is defined and implemented differs and will be explained in greater detail in Chapter 3.

While the absorption based model has a simple inverse solution method to determine what the layer thickness is and therefore what the layer specific spectral contributions for absorption are, the scope of the licentiate thesis here will focus on the forward model case to validate whether this simple, partial volume approach can be validated in experimental data (Chapter 4) and therefore provide a mathematical basis for an iterative inverse solver approach envisioned for the latter half of the PhD project. It is worth noting that, once the top layer thickness is estimated, the layer specific contributions for both the absorption (and now

reduced scattering) spectral can be determined in the same way as proposed in the absorption model.

Chapter 3 Modeling Depth of Interrogation of Detected Light

3.1 Introduction

As alluded to in the previous section there are several simple metrics based on measured tissue optical properties that can provide a basis for estimating the depth at which detected light interacted with tissue. Previous methods had adopted classical penetration depth metrics that have been derived from standard diffusion approximation model solutions to the Radiative Transport Equation [40] or higher order diffusion approximations, such as the delta-P_1 model [41]. Though these are easy to calculate, they presume equal light interaction across its estimated depth into tissue. In a two-layer construct, this tends to underestimate the contribution from the top layer and overestimate contributions from the bottom. While these bias errors were shown to remain relatively small for normal skin, ~15-30 microns, in previous investigations [39], we propose a more advanced approach to estimating depth specific contributions to the detected light signal by describing depth penetrance in terms of fluence.

3.2 Continuous Fluence based model

As fluence describes the non-linear distribution of light in a turbid medium, such as skin, in terms of the bulk absorption and scattering properties present, it can provide a the basis for a potentially more accurate estimate of layer specific contributions in the resulting detected signal. As we are interested estimating the depth distribution of the subset of light remitted from the tissue and not the distribution of light within it (which is what fluence describes), we have adopted a forward-adjoint method. Here the forward contribution describes the fluence entering the tissue and the adjoint contribution, describes the fluence exiting the tissue. Given that SFDI/S is modelled as a planar illumination method, this forward-adjoint approach simplifies to the just taking the square of the fluence. Equations describing depth dependent fluence already exist in several diffusion-based solutions of light transport for planar illumination. For these initial investigations, we have adopted the delta-P_1 solution for fluence described in Carp et.al. [41] and modified for the spatial frequency domain [42].

From these sources, we have proposed a continuous fluence based model to describe the non-linear depth distribution of detected light as follows:

$$Refl_{meas}(z) = \phi^2(z) = (\alpha e^{-\mu_{tr}^* z} + \beta e^{-\mu_{eff} z})^2 \quad (8)$$

Here $Refl_{meas}(z)$ represents the relative contribution to the detected reflectance signal in terms of the depth the light interacted with the tissue. From the delta-P_1 derivation, this depth specific contribution is dependent on the absorption (μ_a) and reduced scattering coefficients (μ_s') of the medium as well as the average spatial frequency used in the SFDI measurement to determine these optical properties. The delta-P_1 transport coefficient, μ_{tr}^*, is defined as: $\mu_{tr}^* = \mu_a + \frac{\mu_s'}{(1-g)}(1-g^2)$, where g is defined as the anisotropy factor, which correlates to the forward directionality of scattering angles and commonly presumed to have a value of 0.8 in tissue and 0.9 in silicone phantoms used in Chapter 4. The effective extinction coefficient includes the depth sensitivity influence of the spatial frequencies (f_x) used and is defined as: $\mu_{eff} = \sqrt{3\mu_a\mu_{tr}^* + 2\pi f_x}$. The scalar weighting coefficients, α and β, balance both boundary conditions for the delta-P_1 with the optical properties present within the medium and are defined by equations 19 and 20 in Carp et.al.[41]

In the two-layer model we proposed in the previous chapter (equation (7)), the partial volume contribution from the top layer, $\alpha(\lambda)$, will take the form of:

$$\alpha(\lambda) = \frac{\int_0^l \phi^2(\lambda, z)\, dz}{\int_0^\infty \phi^2(\lambda, z)\, dz} \quad (9)$$

Where l in this case represents the thickness of the top layer.

3.3 How instrument design impacts depth sensitivity in SFDS

SFDS [25] and SFDI [26], implemented in variety of ways, give the ability to quantify absorption and scattering properties of tissue and other diffusive media in the visible and near infrared ranges [25, 26, 33, 43]. These techniques have shown promise for non-invasively

evaluating malignancies [44, 45], wound severity [46, 47] and tissue viability [48, 49] in skin. Depth sensitivity and subsurface discrimination techniques, which are possible using SFDI/S, are essential components for precise characterization of particular tissue volumes in many of these clinical applications [37, 50-53]. In order to correlate the measured remitted reflectance from turbid media, such as tissue, with precise values of absorption and reduced scattering, spatial frequency domain techniques use the light transport model-based approach.

These models, however, assume a uniform distribution of light, and that the only factors affecting the propagation of this planar illumination pattern are the absorption and scattering characteristics of the tissue volume. In order to separate observed reflectance signals coming from the interaction of various light patterns with tissue itself, the optical design and performance of the instrument must be taken into consideration. As mentioned before, this task is carried out in a calibration technique where a reference phantom with known optical properties is measured either before or after the target medium [25, 26] to characterize the instrument contributions to the measured reflected signals.

However, this approach corrects for any out-of-plane degradation of pattern integrity and the inhomogeneities in the illumination intensity over the field of view at each individual spatial frequency. The first case is a result of the SFDS/I system's optical design, specifically its chromatic aberrations and depth of focus which vary in relation to the ideal picture plane. A digital micromirror device which is tailored for wide field projection applications is normally used in the design process of these systems since many of these systems are constructed around pre-existing projection units [30, 54-57]. As a result, additional lenses are used to reduce the projection field of view but also reducing the working distance between the projection lens and the target to be measured which is beneficial towards small handheld systems in the future. The reduced distance between the target medium and the projection lens affects the depth of focus and blurs the pattern that propagates into the target volume. Similarly, chromatic aberrations can also be problematic because most achromatic designs only correct for this form of aberration over a limited range of wavelengths. It has been demonstrated that errors in the estimation of optical properties may occur when the target tissue has a distinct topology, due to the tissue surface's distance from the ideal imaging plane of the SFDI/S apparatus [58]. Previous studies have also been trying to correct for this displacement error in different ways [53, 59-61]. As different designs exhibit different magnitudes of aberration error, a simplified and straightforward characterization method, that

has been explained in paper no.3 [32] can offer crucial input on the accuracy and spectral integrity of depth specific optical properties. In this paper, I have showed how this data can be used to compensate for such errors for a spatial frequency domain setup, which is susceptible for these kind of errors because of its compact design [Figure 7 (a,d) and Figure 8 (a,d)]. The compensation method is evaluated both in measurement of a phantom with differing optical properties of that used in the characterization [Figure 7 (b,e) and Figure 8 (b,e)], to demonstrate that this empirical method can be applied to arbitrary tissue optical properties and in multilayer phantom constructs [Figure 7 (c,f) and Figure 8 (c,f)], to demonstrate that sub-surface optical properties can be extracted when the top layer properties are known.

To that end, we have characterized the depth dependent contributions due to optical aberrations across the spectral range of the SFDS system we use. As the contributions of these aberrations have been shown to be independent from those of the optical properties of the tissue, this correction factor, $c_{inst}(\lambda,z)$, can be applied as a scaling factor to correct the bottom layer spectra after the layer thickness has been estimated [32].

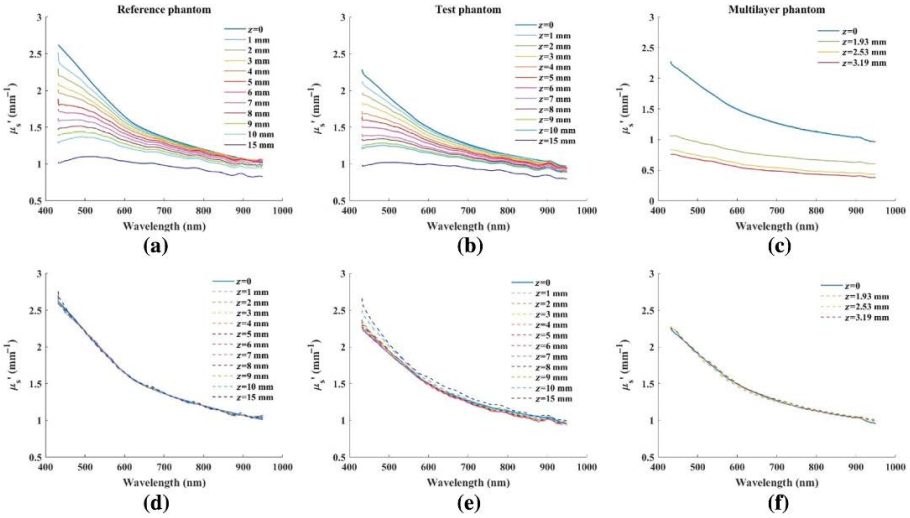

Figure 7 Reduced scattering coefficient calculated at each distance and the respective aberration compensated data for the (a) and (d) reference phantom; (b) and (e) test phantom; and (c) and (f) multi-layered phantoms. z=0 refers to the ideal, in-focus reduced scattering spectra. (Source: *Majedy, M., et al. [32]*)

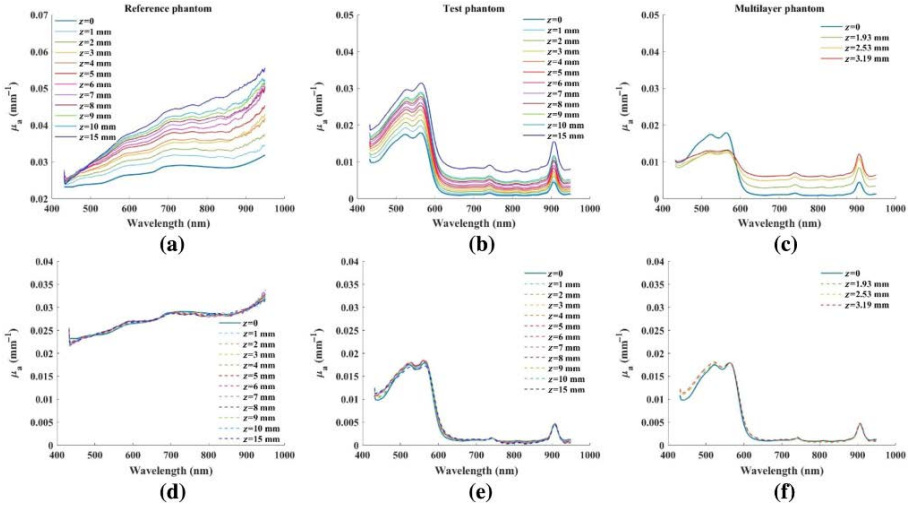

Figure 8 Absorption coefficient calculated at each distance and the respective recovered aberration compensated data for the (a) and (d) reference phantom; (b) and (e) test phantom; and (c) and (f) multi-layered phantoms. z = 0 refers to the ideal, in-focus absorption spectra. (Source: *Majedy, M., et al. [32]*)

Chapter 4: Methods for Independent Validation of Two Layer model – Phantoms and Measurements

4.1 The importance of using optical phantoms before clinical studies

Optical phantoms are an essential tool in the development and validation of optical imaging techniques and equipment. These phantoms are designed to simulate the optical properties of human tissue and are used to test and calibrate the equipment and techniques that will be used in clinical studies. The use of optical phantoms prior to clinical studies is important for several reasons.

First and foremost, working with optical phantoms allows researchers to ensure the accuracy and reliability of the equipment and techniques used in the study. By testing and calibrating the equipment and techniques on phantoms, researchers can identify and correct any issues before conducting the study on live subjects. This can help prevent inaccurate or unreliable results, which can lead to false conclusions about the effectiveness of a treatment or diagnostic technique.

Additionally, optical phantoms provide a way to standardize measurements and techniques across different studies. This is important for ensuring the reproducibility and comparability of results across different studies. By using the same optical phantom in multiple studies, researchers can ensure that the results are comparable and that any differences in results are not due to variations in equipment or techniques.

Furthermore, optical phantoms can help identify and troubleshoot any technical issues with the equipment or techniques before they are used in a clinical setting. This can ensure that the equipment and techniques are in optimal working condition and that any issues can be addressed before they can affect the outcome of the clinical study.

Moreover, using optical phantoms instead of human subjects in initial testing phase can also help to avoid any ethical concerns. This will not only help to protect human subjects from potential harms, but also provide a more reliable way to validate the accuracy of the technique or equipment.

So, working with optical phantoms is important for ensuring the accuracy and reliability of the equipment and techniques used in the study, standardizing measurements, and techniques across different studies, identifying and troubleshooting technical issues, and avoiding ethical concerns. All of these factors can help to ensure that the results of the study are accurate and reliable and can help to avoid false conclusions about the effectiveness of a treatment or diagnostic technique. On the other hand, melanoma and the tumor environment is very complex so if we are going to propose a model, we want to avoid the errors made by drawing false conclusions based on the data and we want to have something independent.
In this work, two phantom models have been developed and investigated:

1- The solid, multilayer silicone (PDMS) phantoms to validate the layer thickness estimation and determine its accuracy over a physiologically relevant range.
2- The liquid hemoglobin phantoms to validate the accuracy and spectral integrity of the layer specific optical properties in terms of hemoglobin concentration and oxygenation accuracy.

I will start with the step-by-step fabrication process for the PDMS phantoms and then go through the liquid hemoglobin phantoms and explain them briefly.

4.2 Multi-layer PDMS phantoms

A step-by-step process for fabricating silicone phantoms adjusted to certain optical properties in the visible and near infrared range is detailed below. This method is both controllable and repeatable [62].

Tissue mimicking phantoms were generated using three main ingredients to get relevant absorption and scattering properties of the dermis: titanium oxide to emulate scattering, red food dye (Dr. Oetker) to emulate the absorption of the underlying properties of skin and approximate hemoglobin absorption and instant coffee approximate the absorption properties of melanin. Optically semi-infinite samples of all these phantoms (homogeneous phantoms >2cm thick) were spectrally characterized independently using spatial frequency-domain spectroscopy (SFDS) measurements.

Figure 9 Images of the components to the multi-layer phantom constructs developed to emulate pigmented nevi at multiple thicknesses. Thin layer samples fabricated with the same concentrations of absorber and scatterer, but at multiple thicknesses based on the volume used (left). Assembly of two-layer construct with coffee phantom layer placed on top of the pink (dermal) phantom (right). All SFDS measurements were collected from 3 central locations within the coffee phantom disk.

4.2.1 Base Layer to emulate underlying dermal properties

As the base medium for these phantoms, raw PDMS silicone and a curing agent are mixed with each other at ratio of 10:1. Scattering was reached using rutile TiO2 powder (Titanium (IV) Oxide, anatase, Sigma-Aldrich). TiO2 is a very effective scatterer because of its high index of refraction [63]. A cream cheese case, which yielded in a solid phantom with the same dimensions was used as a mold for the pink phantom that was designed to emulate the underlying properties of skin. Red food dye was used as an absorber in this phantom. As for the reference calibration phantoms, India Ink was used as an absorber instead. The procedure for how to create these phantoms has been explained in detail elsewhere [62]. This base layer was needed to be thick enough to be greater than the optical penetration depth of the SFDS system, but the exact height was not an important factor in the context of this study.

4.2.2 Fabrication of the thin “melanoma” layer phantoms

Figure 10 illustrates a summary of the process flow which will be described in detail.

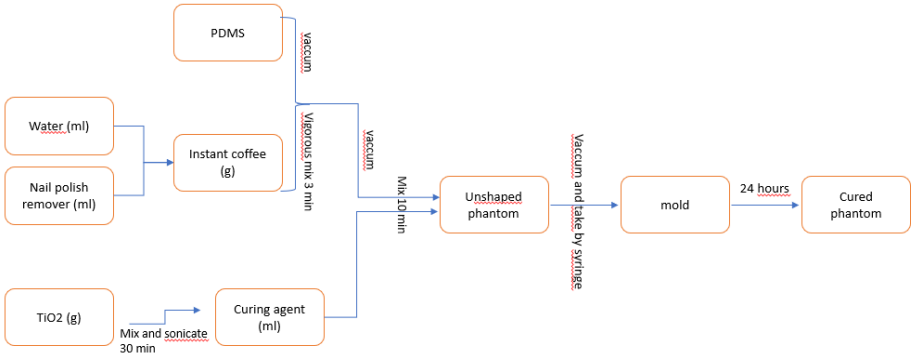

Figure 10 An overview of the key stages involved in creating a phantom.

For the coffee phantoms, a disposable syringe was used to extract 20 mL of curing agent and transfer to a beaker. A variable amount of TiO2 was weighted out for each batch and was added to the curing agent. This solution was mixed by hand and was placed in an ultrasonic bath for 30 minutes. The blend was mixed several times to avoid sedimentation of TiO2. During this 30-minute period, 200 ml PDMS was placed into a plastic beaker. It was then placed in the vacuum for 5 minutes. A variable amount of instant coffee was measured by weight and was mixed with 0.25 ml water to make a runny paste. 0.15 ml nail polish remover was added to this paste to make it easier to mix with the PDMS by swelling it by a small extent. The coffee solution was then added to the PDMS and was mixed by hand vigorously for 10 min before placing it in vacuum for the rest of the time. The silicone mixed material was injected into the petri dishes for different thicknesses of coffee phantoms using 1 ml insulin syringes in 0.5, 1, 1.5, 2, 2.5, and 3-ml volume. As a result of excess silicone left in the syringes in each try the thickness varied by +/- 0.03 mm.

The bubbles that build up during the curing process at the top of the phantom during the first minutes of the curing process were punctured using a sharp object to make sure there were no imperfections in the phantom. These phantoms were cured in the room temperature in 24 hours. The reproducibility of the process has been investigated before [62].

4.2.3 Initial results from these multi-layer phantom measurements:

As stated in Chapter 2, one limitation of the absorption-based model was the depth in which the light could probe the tissue. Melanin absorption will impact the light penetration as a function of wavelength since it is highly absorbing in the visible regime and not so much in the NIR. So, the penetration depth becomes incrementally deeper and deeper when encountering a heavily melanized tissue. Scattering within the melanized tissue is different from the dermal scattering. So, we can utilize the depth penetration estimate and separate the scattering properties of each layer.

Based on the volume of the coffee in the petri dishes in these multi-layer phantom measurements, we can fabricate various layer thicknesses and stack them on the top of each other and see how the light penetrates through one layer into the next and how that impacts the scattering properties of each layer.

One example from these phantom measurements is Figure 11, where the blue line shows the reduced scattering coefficient of the dermal phantom alone and the brown line is the reduced scattering coefficient from all the coffee phantoms. The spectra between these homogenous reference cases are the reduced scattering coefficient from different thicknesses of coffee phantoms on the top of the dermal phantom.

These measurements show that in the multi-layered phantom constructs (thin coffee phantoms on the top of the pink phantom emulating dermal tissue of the skin) the scattering properties of the thin layers of coffee phantom are closer to the bottom layer and the thicker it gets the closer to the scattering of the coffee phantom.

The transition in between it indicates the “meter stick” approach of transition from one layer scattering properties to the other. Once we decouple the scattering from one layer versus the other and with having a greater specificity of where the scattering is coming from, we can look at the signals and where it comes from based on density and size of the objects and use the scattering properties of the lesion to estimate the thickness of the coffee phantom.

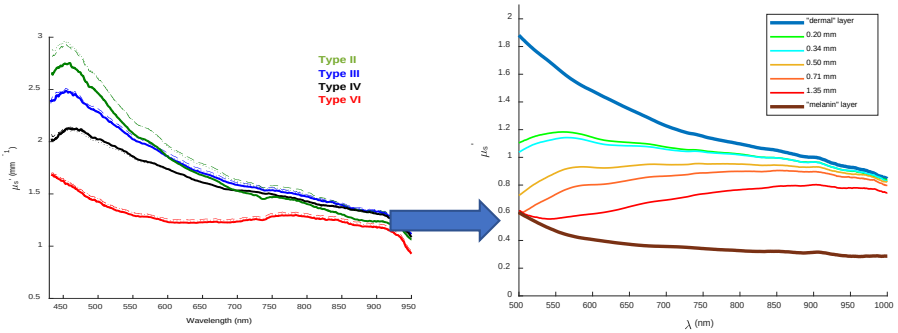

Figure 11 On the left is series of scattering spectra measured across four healthy skin types ranging from I-IV on the Fitzpatrick scale as reported in . This left figure is included to provide context to the measured results from a series of tissue simulating phantoms with "melanoma" layers ranging from 0.2-1.35mm.

4.3 Liquid hemoglobin phantoms

Three different types of hemoglobin -Whole Blood (WB), Lysed Blood (LB), and a powdered, freeze-dried form of human hemoglobin (A0) - were used to create liquid phantoms. These samples were first examined using SCT in both their oxygenated and deoxygenated states after being combined with a yeast solution. Afterwards, the three hemoglobin preparations were blended with Intralipid, which served as a scattering agent, to create phantoms that mimic tissue.

The blood samples were obtained from the Linköping University Hospital and were collected according to the guidelines set forth by the Swedish act SFS 2003:460 and the Declaration of Helsinki. Participants' identities were kept confidential, and they provided both oral and written consent. The blood was stored in vacuum tubes coated with heparin until it was used for the experiments. In the case of WB, 3 ml of the blood sample was diluted with deionized water for each individual experiment. For LB, the blood was centrifuged at 500 g for 5 minutes to separate the cell and plasma components, with the plasma and buffy coat being removed and discarded. The erythrocyte pellet was then suspended in 5 ml of phosphate-buffered saline and centrifuged again at 500 g for 5 minutes to pellet the cells. The supernatant was discarded, and a solution of sterile water was added to the pellet. The osmotic pressure difference between saline and water causes the erythrocytes to lyse. After the sample was centrifuged at 2000 g for 5 minutes to pellet the cell membrane fragments and create a clear lysed erythrocyte fraction the lysis was allowed to proceed for 5 minutes at room

temperature. LB was then mixed with deionized water and left overnight to allow for further sedimentation of insoluble fragments and debris. For the third preparation, a powdered, freeze-dried form of human hemoglobin A0 (H0267 ferrous-stabilized, Sigma Co., St. Louis, Missouri) was dissolved in deionized water at a concentration of 8mg/ml.

As for the tissue-Mimicking Liquid Phantoms, in order to create the liquid phantoms with a tissue-like optical properties, a mixture of 15 ml of 20% Intralipid solution (Fresenius Kabi AB, Uppsala, Sweden) and 185 ml PBS was prepared. This resulted in a reduced scattering coefficient of approximately 2.5mm-1 at 550 nm. For each type of hemoglobin preparation, 3 ml of undiluted WB, lysed hemoglobin, and 80 mg of ferrous stabilized hemoglobin were added to the Intralipid mixture. The phantoms were heated to maintain a constant temperature of around 34°C. Prior to data collection, the phantoms were oxygenated for 20 minutes using a magnetic stirrer to ensure complete oxygenation of the hemoglobin. These liquid phantoms are explained in detail in the paper no.2.

4.3.1 Key Results from these phantoms

I will summarize the main results of the research on liquid hemoglobin in this section, but for a more detailed analysis, please refer to the papers included at the end of this thesis.

In this study, the absorption spectra of three hemoglobin solutions were analyzed and characterized using a technique called spectroscopic collimated transmission (SCT). These solutions included whole blood, lysed blood and ferrous stabilized hemoglobin. Tissue mimicking phantoms were created by combining Intralipid with the hemoglobin solutions and were studied using spatial frequency-domain spectroscopy (SFDS) and enhanced perfusion and oxygen saturation (EPOS). Oxygen depletion was accomplished by adding yeast to the phantoms.

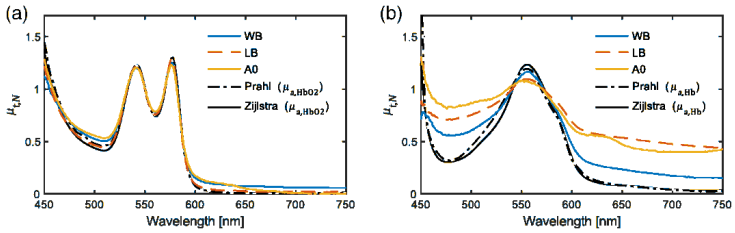

Figure 12 The total attenuation coefficient (μ_t) of white blood cells (WB), red blood cells (LB), and ferrous-stabilized hemoglobin (A0) was measured in both oxygenated (HbO2) and deoxygenated (Hb) samples using the SCT setup. The results were normalized and compared to reference absorption spectra from previous studies by Prahl and Zijlstra et al. (Source: Majedy, M., et al. [33]).

This study compares the results from the SCT measurements to reference spectra from two other sources to validate the results. The study found that the three hemoglobin preparations exhibit similar absorption spectra with slight differences in total attenuation coefficient. The study also found that when fitting to reference spectra from Prahl, Zijlstra et al., and the optimal combination of these (Prahl for oxyhemoglobin and Zijlstra et al. for deoxyhemoglobin) that the estimated oxygen saturation for the three preparations were at 96% to 97% which were slightly lower than the expected 100%.

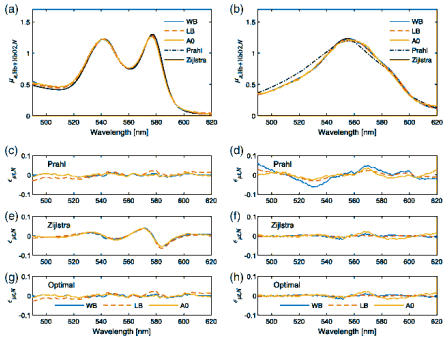

Figure 13 The absorption spectra of hemoglobin (Hb+HbO2) were measured and normalized using the SCT method, accounting for the absorption and scattering of methemoglobin. The results were compared to reference spectra from previous studies by Prahl for oxyhemoglobin preparations and by Zijlstra et al. for deoxyhemoglobin preparations. The residual spectra from these comparisons were also analyzed, including the use of optimal reference spectra for oxyhemoglobin from Prahl and for deoxyhemoglobin from Zijlstra et al. (Source: Majedy, M., et al. [33])

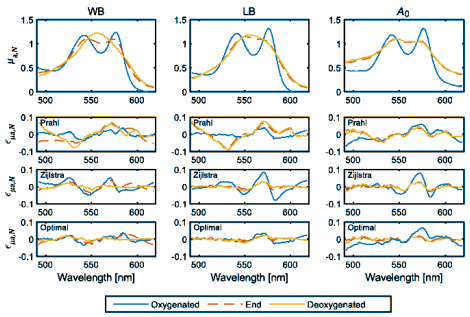

Figure 14 The absorption spectra of white blood cells (WB), red blood cells (LB), and ferrous-stabilized hemoglobin (A0) were measured using SFDS on tissue-mimicking phantoms containing Intralipid and hemoglobin. The data includes absorption spectra for oxygenated hemoglobin (HbO2), deoxygenated hemoglobin (Hb) in bulk media, and deoxyhemoglobin at a specific time point (End) where a thin plastic film was used to prevent surface oxygenation. The results were normalized and compared to reference spectra from previous studies by Prahl, Zijlstra et al., and the optimal set of reference spectra. The residual spectra from these comparisons were also calculated. *(Source: Majedy, M., et al. [33])*

The study aimed to determine the relative advantages and disadvantages of each method, including their spectral properties, cost, access, complexity, and desired use. The study found that while freeze-dried ferrous-stabilized human hemoglobin is commercially available and poses no risk of blood-borne pathogens, it also contains methemoglobin, which can vary depending on the source and storage conditions. It was also found that WB-based hemoglobin exhibited near-equivalent spectral characteristics as lysed hemoglobin, apart from a small contribution of scattering due to the presence of intact erythrocytes. LB was found to provide the best match to reference spectra of both oxy- and deoxyhemoglobin and does not have the issues of additional methemoglobin contamination or scattering present in WB and WB shares the same issues of access and safe handling as LB and it has greater complexity in this process and greater risk for potential blood-borne pathogen exposure.

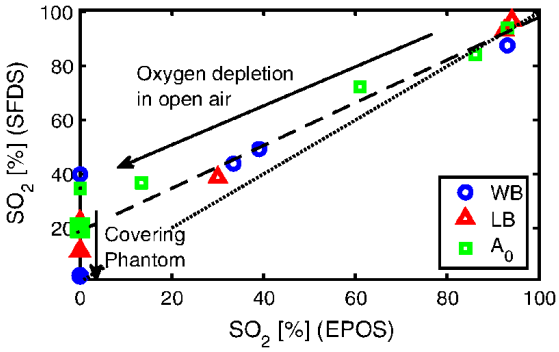

Figure 15 The SFDS method was used to measure the oxygen saturation (SO2) of white blood cells (WB), red blood cells (LB), and ferrous-stabilized hemoglobin (A0) simultaneously at the surface of a phantom and compared to the values obtained by EPOS (submerged about 2 cm). The results are represented by markers, filled markers indicate SO2 values measured about 5 to 10 minutes after a plastic film covered the surface of the phantom. The discrepancy in the rate of oxygenation change (24%) is shown by the difference in slope between the dashed line and the dotted line (which represents unity). (Source: Majedy, M., et al. [33])

Chapter 5: Review of papers

The three papers (two peer reviewed publications and an accepted conference proceeding) on which the thesis is based are reviewed below, including description of the author's contribution to each paper.

5.1 Paper I (Proceeding): **Evaluation of Tabulated Hemoglobin Absorption Spectra Using Collimated Transmission on Oxygenated Human Lysed Blood**

Majedy, Motasam, Marcus Larsson, and Göran Salerud. "Evaluation of tabulated hemoglobin absorption spectra using collimated transmission on oxygenated human lysed blood." In European Conference on Biomedical Optics, pp. ES2B-6. Optical Society of America, 2021.

Blood oxygen saturation is a crucial component of patient diagnosis, monitoring, and treatment follow-up in clinical settings.
Quantifying the relative amount of oxygenized hemoglobin using spectroscopic optical methods is one method of determining the level of oxygen in blood.
The algorithms behind many of these techniques are derived from tabulated data on the absorption coefficient of oxygenated and reduced hemoglobin that Prahl et al. and Zijlstra et al. published.

In this work, absorption coefficient of oxygenated human lysed blood was evaluated with collimated transmission to estimate blood oxygen saturation using tabulated hemoglobin absorption spectra. It was found that both sets show good conformity but also minor differences that can impact the accuracy of the estimations. The model based on Prahl's data produced consistently lower errors. This suggests that when developing inverse algorithms for quantifying blood oxygenation, the Prahl's oxyhemoglobin spectrum should be used.
However, both the Zijlstra and Prahl models estimated SO2 levels in the 90-96% range, rather than the expected 100%, which is consistent with previously reported phantom experiments.

Author's Contribution

Contributed to the idea, designed the experiments, acquired all data, and performed all the analysis for this presentation and proceeding. I was primarily responsible for writing the entire manuscript.

5.2 Paper II: **Spectral characterization of liquid hemoglobin phantoms with varying oxygenation states**

Majedy, Motasam, Rolf B. Saager, Tomas Strömberg, Marcus Larsson, and Göran E. Salerud. "Spectral characterization of liquid hemoglobin phantoms with varying oxygenation states." Journal of Biomedical Optics 27, no. 7 (2021): 074708.

The article discusses the importance of accurately measuring hemoglobin oxygen saturation (SO2) in the body and the need for reliable methods to calibrate devices used for this purpose. The author proposes the use of three different liquid hemoglobin preparations (whole blood (WB), lysed blood (LB), and ferrous-stabilized hemoglobin) in tissue-mimicking phantoms and evaluate their absorption spectra using various spectroscopic techniques and considers factors such as cost, access, complexity, and intended use. The results showed that all three preparations exhibited similar absorption spectra, but differences were observed in the fitting depending on the reference spectra used. The author also found that constant stirring is critical for the accuracy of SO2 measurements using WB, and that there are difficulties with access and handling for both WB and LB. The ferrous-stabilized hemoglobin had the advantage of being commercially available and not posing a risk of blood-borne pathogens, but it was found to contain methemoglobin. It was also found that measurements taken using spatial frequency-domain spectroscopy (SFDS) on the surface of the phantoms were affected by oxygen diffusion at the air interface, leading to higher values compared to measurements taken using the enhanced perfusion and oxygen saturation (EPOS) system. The article concludes by highlighting the importance of properly characterizing blood phantoms and considering the specific considerations required for each type.

Author's Contribution

Contributed to the idea, designed the experiments, acquired all data and performed all the analysis for the paper. I was primarily responsible for writing the entire manuscript but accepted contributions from co-authors in the introduction and discussion sections.

5.3 Paper III: **Influence of optical aberrations on depth-specific spatial frequency domain techniques**

Majedy, Motasam, Nandan K. Das, Johannes Johansson, and Rolf B. Saager. "Influence of optical aberrations on depth-specific spatial frequency domain techniques." Journal of Biomedical Optics 27, no. 11 (2022): 116003.

Spatial frequency domain techniques use spatially modulated illumination patterns to quantify absorption and scattering properties of tissue and other diffusive media across visible and/or near-infrared ranges. Through the quantification of these optical properties, SFDI/S has demonstrated the potential to non-invasively assess skin cancers, wound severity, and tissue structure and viability in the skin. In many of these clinical applications, such as burn wound assessment and melanin quantification, depth sensitivity and subsurface discrimination approaches enabled by SFDI/S are critical features toward accurate characterization of specific tissue volumes. Spatial frequency domain techniques utilize a light transport model-based approach to relate the measured remitted reflectance from turbid media, such as tissue, to quantitative values of absorption and reduced scattering.

These existing models presume a uniform distribution of light upon which the spatial frequencies are encoded, and the propagation of this planar illumination pattern will only be impacted by the absorption and scattering properties within the tissue volume. To that end, the optical characteristics of the instrument must be accounted for to isolate measured reflectance signals resulting from the interaction of these illumination patterns with the tissue itself. Though not often acknowledged explicitly in the literature, this calibration approach using

turbid reflectance standards not only will correct for inhomogeneities in illumination intensity over the field of view at each individual spatial frequency, but also any out-of-plane degradation of the pattern integrity as the planar illumination pattern propagates into the tissue volume. This could rapidly blur the projected pattern as it propagates into the tissue volume and compete with the effects of light scattering.

It has been shown that when the target tissue has a distinct surface shape and depth, errors in the determination of optical properties may occur due to the tissue surface's distance relative to the ideal imaging plane of the SFDI/S instrument.

In this work, we will present a simple method using a single tissue-simulating phantom to evaluate the influence of out-of-plane optical aberrations in the context of the resulting absorption and reduced scattering coefficients. Additionally, once this optical characterization is obtained, we will also demonstrate how this data can be used to compensate for these aberration errors in post-processing for a spatial frequency domain setup that is particularly susceptible to these types of aberrations. The former one demonstrates that this empirical method can be applied to arbitrary tissue optical properties over a range of positional displacements from the ideal image plane and in the latter case demonstrates that sub-surface optical properties can be extracted when the top layer properties are known.

Author's Contribution

Performed all data acquisition and analysis for this paper. I contributed to the experimental design and modeling approach with the final author. I was primarily responsible for writing the entire manuscript.

Chapter 6: Discussion and Future Work

Given the highly visual nature of current screening methods as the ABCDE method, it is quite obvious that there would be several opportunities that optical methods could serve as a means to improve both the sensitivity, but more importantly the specificity of this initial stage of early melanoma detection. Any improvement in the initial screening process would have many downstream benefits. Greater sensitivity at early stages of Melanoma could improve survival rates, but greater specificity could dramatically reduce the number of unnecessary biopsies. This latter improvement has several, often unrecognized, beneficial consequences. First, a reduction in number of biopsies would reduce the cost and healthcare burden. Second, it would also positively impact the mental health of patients, particularly those at high risk as there is often 1-2 weeks between the screening where biopsies are taken and the confirmation as to whether the patient may have melanoma or not. In addition to the discomfort felt from the biopsy, this lag in time can produce uncertainty and anxiety in the individual. Given that there is such a high rate of negative (benign) results, patients, particularly those at high risk, may lose confidence in the effectiveness of the current screening process and hence avoid future screenings and care. Over all the well intentioned efforts in developing spectroscopic imaging tools over the past 20 years, however, little progress has been made towards clinical impact and the subjective, clinician-dependent ABCDE method remains a clinical screening standard. The motivation of this research effort is to first understand why optical methods have been unable to gain such clinical acceptance and try to define in more conclusive terms what limitations and challenges remain in their way.

In the context of this thesis, the first challenge we have identified is the need to isolate optical properties from specific volumes of tissue to avoid confounding artefacts due to spectral depth penetrance and partial volume effects. The SFDS technique would give quantitative, functional information about the specific chromophores present in each layer of the tissue. Using this technique and as a part of a bigger project, we propose the implementation of a two-layer model that utilizes the scattering contrast between melanized tissue and the dermis. Scattering is advantageous in a spectral layered model because its relatively featureless power law shape can be leveraged to estimate the thickness of layers at greater depths than would be possible with absorption-based models. One of the key benefits is its ability to estimate layer thicknesses in a continuous manner, while also considering the impact of partial volume

effects. Moreover, it can estimate thicknesses in the visible and near infrared spectrum, potentially reaching a maximum thickness of 3-4mm.

The proposed two-layer model based on scattering contrast is heavily dependent on robust estimations of the fractional contributions of the two layers relative to the depth and distribution of spatial frequency dependent signals detected at every wavelength. Previous two-layer model approaches have used simple depth penetrance metrics as a means to differentiate the respective volumes of healthy skin measured in the visible and near infrared regime [38, 39]. In the case of thicker tissue volume ranges, as expected in melanoma screening, however, these simple metrics may not be sufficient to accurately differentiate contributions from both layers. To that end, we have developed a new, continuous distribution metric based on models of fluence instead. Not only can this describe the non-linear distribution of light within tissue depths, utilizing the delta-P_1 solution, we can describe in an analytical expression to a greater degree of accuracy than the standard diffusion approximation. While a Monte Carlo solution remains the current gold standard for describing light transport in tissue, these solutions lack the speed and flexibility of analytic expressions and using Monte Carlo to describe continuous fluence in the spatial frequency domain has remained unrealized. Currently only rough percentile estimations of spatial frequency depth estimations have been demonstrated [64]. The result of SFDS system's optical design, specifically the chromatic aberrations and depth of focus, are also important to be considered. This is a unique contribution of this thesis work to the much broader SFDI research community as we are the first to characterize how lens design and optical aberrations can impact the depths this imaging approach can achieve in tissue, independent from the optical properties contained within these tissue volumes. Careful characterization of these instrument specific aberrations can hence improve the depth estimation of layers within tissue, but also correct the spectral distortion these aberrations can imprint on the subsurface tissue spectra.

It is essential to independently evaluate a technique before utilizing it with clinical data because independent validation and characterization helps to ensure that the technique is accurate and reliable. One way to achieve this is by using optical phantoms, which provide a controlled and known environment that allows for accurate and precise measurements of the technique's performance. These measurements can be used to establish the technique's accuracy, precision, and reliability, which can be compared to the performance of other

techniques. Additionally, using phantoms can help identify and troubleshoot any potential issues with the technique before it is used with clinical data, which is often limited in terms of sample size and volume and might not provide an accurate representation of the technique's performance. Furthermore, in clinical practice, the results are more complex than in controlled conditions, and other factors such as patient's condition, and other parameters can affect the performance of the technique. By independently evaluating the technique using phantoms, researchers can ensure that the technique is robust and reliable before it is used in clinical settings, increasing the chances of accurate and reliable results. To this end, we have developed two distinct types of phantoms to target specific challenges in imaging pigmented nevi and use them as a controlled and independently verifiable platform to determine the accuracy of this (and any other) layered model approach to isolate layer thicknesses and the respective spectral properties (multi-layer PDMS phantoms) and then also determine the accuracy and spectral integrity of the underlying tissue when interpreted in terms of physiologic properties, such as oxy- vs deoxyhemoglobin concentrations (liquid hemoglobin phantoms with coffee-layer phantoms place on top)

By learning from the limitations of previous optical imaging approaches and disentangling confounding sources that impact the measured spectra from tissue, we aim to evaluate several new and depth specific parameters that could substantially improve current screening practices. The assessment of melanin depth distribution could act as a non-invasive estimate of the Breslow Depth and Clark Scale. While this parameter alone may not effectively serve as a diagnostic biomarker for melanin, this parameter could greatly assist in monitoring suspicious, yet superficial nevi over time. This depth distribution could be tracked over screenings to monitor and evolution of the nevi and hence result in a biopsy only when there is an indication of growth and invasion. Isolation of the layer specific melanin absorption could provide a more robust evaluation of the question regard whether the molecular structure of melanin becomes altered in melanoma. The idea of using a shift in the melanin spectrum had been proposed in previous spectral techniques as a potential diagnostic marker for cancer [36], however, these early techniques were susceptible to partial volume effects which also can produce similar shifts in the measured data. With the layer specific absorption isolated, this idea can be revisited and evaluated. Lastly, the isolation of layer specific scattering can now provide previously unexplored opportunities to evaluate whether morphologic changes within cancerous tissue, typically assessed microscopically through histology, could be characterized over wide fields of view. The spectral scattering properties are dependent on

the density and size distributions of microscopic features [65], like nuclei, mitochondria, lysosomes, collagen bundles and fibrils, etc. By isolating the depth specific scattering, there may be a new optical biomarker that can use these spectra to characterize and potentially differentiate local tissue morphology between cancerous and benign lesions.

Future work

Once this new model of scattering based tissue discrimination can be rigorously validated in a forward model sense (Paper IV) an inverse solver strategy will need to be developed (Paper V). To start, we will explore iterative methods utilizing non-linear fitting, utilizing adjacent, non-pigmented (normal) skin as a reference for underlying scattering properties. This strategy is a simple, pragmatic approach to assist in minimizing free parameters and iterations in the minimization approach.

Once a method of layer thickness can be established, the value and impact of the localized tissue optical properties can be explored. Critical to this exploration is a priori establishment of any model-based errors to avoid over-interpretation of the spectral data (and its diagnostic potential) derived from in vivo data (Paper V). Given that there are far more benign pigmented lesions that are suspected as potential melanomas under current clinical practice, it would be anticipated that any clinical study employing optical techniques, like what we propose, could become biased due to the imbalance between benign and melanoma data. However, with the further development of more advanced tissue simulating phantoms based in preliminary clinical results will help identify whether clinical results would be limited by the sample size and distribution or by the independently validated accuracy of the spectral imaging technique.

Conclusion

This Licentiate Thesis lays the foundational framework to address the unresolved challenge of improving early detection of Melanoma though spectral imaging techniques. These challenges we have identified here all revolve around the need for layer specific imaging. This thesis

proposes a simple two-layer model based on scattering contrast between melanized tissue and the dermis beneath it. The advantage of this approach is that, as a continuous model of partial volume effects, it can estimate layer thicknesses across the entire visible and near infrared spectrum and therefore cover a theoretical range of thicknesses up to 3-4mm. As scattering is the source of contrast, there is also no need to presume chromophores presented in tissue prior to the isolation of depth dependent spectral properties. As modeling the wavelength dependent depth sensitivity and distribution of detected light is critical to this two-layer model, this thesis has also examined other factors outside to the tissue itself that can impact this sensitivity. Lastly, this thesis has developed specialized tissue simulating phantoms to address the need for independent, traceable standards that emulate tissue properties and geometries and establish the performance and accuracy of an imaging technique before it is used in any clinical investigation.

References

1. Bray, F., et al., *Global cancer statistics 2018: GLOBOCAN estimates of incidence and mortality worldwide for 36 cancers in 185 countries.* CA: A Cancer Journal for Clinicians, 2018. **68**(6): p. 394-424.
2. Foundation), C.S.C. *Cancer statistics*. Available from: https://www.cancerfonden.se/om-cancer/statistik.
3. Kappes, U.P., et al., *Short- and long-wave UV light (UVB and UVA) induce similar mutations in human skin cells.* J Invest Dermatol, 2006. **126**(3): p. 667-75.
4. Saginala, K., et al., *Epidemiology of Melanoma.* Med Sci (Basel), 2021. **9**(4).
5. Conforti, C. and I. Zalaudek, *Epidemiology and Risk Factors of Melanoma: A Review.* Dermatol Pract Concept, 2021. **11**(Suppl 1): p. e2021161S.
6. Sung, H., et al., *Global Cancer Statistics 2020: GLOBOCAN Estimates of Incidence and Mortality Worldwide for 36 Cancers in 185 Countries.* CA: A Cancer Journal for Clinicians, 2021. **71**(3): p. 209-249.
7. *International Agency for Research on Cancer*. [cited 2022 27 July]; Available from: https://gco.iarc.fr/today/home
8. Society, A.C. *Melanoma Skin Cancer*. [cited 2022 27 July]; Available from: https://www.cancer.org/cancer/melanoma-skin-cancer.
9. Gandini, S., et al., *Meta-analysis of risk factors for cutaneous melanoma: II. Sun exposure.* European Journal of Cancer, 2005. **41**(1): p. 45-60.
10. Yagerman, S. and A. Marghoob, *Melanoma patient self-detection: a review of efficacy of the skin self-examination and patient-directed educational efforts.* Expert Review of Anticancer Therapy, 2013. **13**(12): p. 1423-1431.
11. Brunssen, A., et al., *Impact of skin cancer screening and secondary prevention campaigns on skin cancer incidence and mortality: A systematic review.* J Am Acad Dermatol, 2017. **76**(1): p. 129-139.e10.
12. Lartigau, E., et al., *Intratumoral oxygen tension in metastatic melanoma.* Melanoma Research, 1997. **7**(5): p. 400-406.
13. Liu, Y., et al., *Targeting hypoxia-inducible factor-1alpha with Tf-PEI-shRNA complex via transferrin receptor-mediated endocytosis inhibits melanoma growth.* Mol Ther, 2009. **17**(2): p. 269-77.
14. Corrie, P.G., B. Basu, and K.A. Zaki, *Targeting angiogenesis in melanoma: prospects for the future.* Ther Adv Med Oncol, 2010. **2**(6): p. 367-80.
15. TANAKA, M., *Dermoscopy.* The Journal of Dermatology, 2006. **33**(8): p. 513-517.
16. Melafind. *Melafind Optical Scanner*. [cited 2022 27 July]; Available from: https://ocaneq.com/melafind.
17. Elbaum, M., et al., *Automatic differentiation of melanoma from melanocytic nevi with multispectral digital dermoscopy: a feasibility study.* J Am Acad Dermatol, 2001. **44**(2): p. 207-18.
18. Claridge, E., et al. *SPECTROPHOTOMETRIC INTRACUTANEOUS IMAGING (SIASCOPY): METHOD AND CLINICAL APPLICATIONS*. 2006.
19. Cotton, S., *A Non-Invasive Imaging System For Assisting in the Diagnosis of Malignant Melanoma.* 1998.
20. Watson, T., et al., *Learning a novel technique to identify possible melanomas: are Australian general practitioners better than their U.K. colleagues?* Asia Pacific Family Medicine, 2009. **8**(1): p. 3.
21. Diebele, I., et al., *Clinical evaluation of melanomas and common nevi by spectral imaging.* Biomedical Optics Express, 2012. **3**(3): p. 467-472.

22. Vasefi, F., et al., *Multimode optical dermoscopy (SkinSpect) analysis for skin with melanocytic nevus*. SPIE BiOS. Vol. 9711. 2016: SPIE.
23. Gioux, S., A. Mazhar, and D.J. Cuccia, *Spatial frequency domain imaging in 2019: principles, applications, and perspectives.* J Biomed Opt, 2019. **24**(7): p. 1-18.
24. Tseng, S.-H., A. Grant, and A. Durkin, *In vivo determination of skin near-infrared optical properties using diffuse optical spectroscopy.* Journal of Biomedical Optics, 2008. **13**(1): p. 014016.
25. Saager, R., D. Cuccia, and A. Durkin, *Determination of optical properties of turbid media spanning visible and near-infrared regimes via spatially modulated quantitative spectroscopy.* Journal of Biomedical Optics, 2010. **15**(1): p. 017012.
26. Cuccia, D.J., et al., *Quantitation and mapping of tissue optical properties using modulated imaging.* J Biomed Opt, 2009. **14**(2): p. 024012.
27. Angelo, J.P., et al., *Review of structured light in diffuse optical imaging.* J Biomed Opt, 2018. **24**(7): p. 1-20.
28. Alwin, K. and S.P. Michael, *Determination of the optical properties of turbid media from a single Monte Carlo simulation.* Physics in Medicine & Biology, 1996. **41**(10): p. 2221.
29. Swartling, J., et al., *Accelerated Monte Carlo models to simulate fluorescence spectra from layered tissues.* J Opt Soc Am A Opt Image Sci Vis, 2003. **20**(4): p. 714-27.
30. Belcastro, L., et al., *Handheld multispectral imager for quantitative skin assessment in low-resource settings.* J Biomed Opt, 2020. **25**(8): p. 1-12.
31. Jonasson, H., C.D. Anderson, and R.B. Saager, *Water and hemoglobin modulated gelatin-based phantoms to spectrally mimic inflamed tissue in the validation of biomedical techniques and the modeling of microdialysis data.* J Biomed Opt, 2022. **27**(7).
32. Majedy, M., et al., *Influence of optical aberrations on depth-specific spatial frequency domain techniques.* J Biomed Opt, 2022. **27**(11).
33. Majedy, M., et al., *Spectral characterization of liquid hemoglobin phantoms with varying oxygenation states.* J Biomed Opt, 2021. **27**(7).
34. Chung, S.H., et al., *Tissue bound water studies on breast tumors using diffuse optical spectroscopy*. SPIE BiOS. Vol. 6434. 2007: SPIE.
35. Marchesini, R., A. Bono, and M. Carrara, *In vivo characterization of melanin in melanocytic lesions: spectroscopic study on 1671 pigmented skin lesions.* J Biomed Opt, 2009. **14**(1): p. 014027.
36. Zonios, G., et al., *Melanin absorption spectroscopy: new method for noninvasive skin investigation and melanoma detection.* J Biomed Opt, 2008. **13**(1): p. 014017.
37. Saager, R., et al., *Method for depth-resolved quantitation of optical properties in layered media using spatially modulated quantitative spectroscopy.* Journal of Biomedical Optics, 2011. **16**(7): p. 077002.
38. Saager, R.B., et al., *Method for depth-resolved quantitation of optical properties in layered media using spatially modulated quantitative spectroscopy.* J Biomed Opt, 2011. **16**(7): p. 077002.
39. Saager, R.B., et al., *In vivo measurements of cutaneous melanin across spatial scales: using multiphoton microscopy and spatial frequency domain spectroscopy.* J Biomed Opt, 2015. **20**(6): p. 066005.
40. Jacques, S.L., *How tissue optics affect dosimetry of photodynamic therapy.* J Biomed Opt, 2010. **15**(5): p. 051608.
41. Carp, S.A., S.A. Prahl, and V. Venugopalan, *Radiative transport in the delta-P1 approximation: accuracy of fluence rate and optical penetration depth predictions in turbid semi-infinite media.* J Biomed Opt, 2004. **9**(3): p. 632-47.
42. Seo, I., C.K. Hayakawa, and V. Venugopalan, *Radiative transport in the delta-P1 approximation for semi-infinite turbid media.* Med Phys, 2008. **35**(2): p. 681-93.
43. Cuccia, D.J., et al., *Modulated imaging: quantitative analysis and tomography of turbid media in the spatial-frequency domain.* Optics Letters, 2005. **30**(11): p. 1354-1356.

44. Rohrbach, D.J., et al., *Preoperative mapping of nonmelanoma skin cancer using spatial frequency domain and ultrasound imaging.* Acad Radiol, 2014. **21**(2): p. 263-70.
45. Saager, R.B., et al., *A Light Emitting Diode (LED) Based Spatial Frequency Domain Imaging System for Optimization of Photodynamic Therapy of Nonmelanoma Skin Cancer: Quantitative Reflectance Imaging.* Lasers in Surgery and Medicine, 2013. **45**(4): p. 207-215.
46. Nguyen, J.Q., et al., *Spatial frequency domain imaging of burn wounds in a preclinical model of graded burn severity.* J Biomed Opt, 2013. **18**(6): p. 66010.
47. Ponticorvo, A., et al., *Spatial Frequency Domain Imaging (SFDI) of clinical burns: A case report.* Burns Open, 2020. **4**(2): p. 67-71.
48. Sun, Z., et al., *Spatial-Frequency Domain Imaging: An Emerging Depth-Varying and Wide-Field Technique for Optical Property Measurement of Biological Tissues.* Photonics, 2021. **8**(5): p. 162.
49. Yang, B., et al., *Polarized light spatial frequency domain imaging for non-destructive quantification of soft tissue fibrous structures.* Biomedical Optics Express, 2015. **6**(4): p. 1520-1533.
50. Konecky, S.D., et al., *Quantitative optical tomography of sub-surface heterogeneities using spatially modulated structured light.* Optics Express, 2009. **17**(17): p. 14780-14790.
51. Mazhar, A., et al., *Implementation of an LED based Clinical Spatial Frequency Domain Imaging System.* Proceedings of SPIE - The International Society for Optical Engineering, 2012. **8254**: p. 8.
52. Sharif, S.A., et al., *Noninvasive clinical assessment of port-wine stain birthmarks using current and future optical imaging technology: a review.* British Journal of Dermatology, 2012. **167**(6): p. 1215-1223.
53. Zhao, Y., et al., *Angle correction for small animal tumor imaging with spatial frequency domain imaging (SFDI).* Biomedical Optics Express, 2016. **7**(6): p. 2373-2384.
54. Applegate, M., et al., *OpenSFDI: an open-source guide for constructing a spatial frequency domain imaging system.* J Biomed Opt, 2020. **25**(1): p. 1-13.
55. Nadeau, K., et al., *Component and system evaluation for the development of a handheld point-of-care spatial frequency domain imaging (SFDI) device*. SPIE BiOS. Vol. 8573. 2013: SPIE.
56. Saager, R.B., et al., *Portable (handheld) clinical device for quantitative spectroscopy of skin, utilizing spatial frequency domain reflectance techniques.* Review of Scientific Instruments, 2017. **88**(9): p. 094302.
57. Strömberg, T., et al., *Spatial frequency domain imaging using a snap-shot filter mosaic camera with multi-wavelength sensitive pixels*. SPIE BiOS. Vol. 10467. 2018: SPIE.
58. Bodenschatz, N., et al., *Sources of errors in spatial frequency domain imaging of scattering media.* Journal of Biomedical Optics, 2014. **19**(7): p. 071405.
59. Gioux, S., et al., *Three-dimensional surface profile intensity correction for spatially modulated imaging.* Journal of Biomedical Optics, 2009. **14**(3): p. 034045.
60. Paquit, V., et al., *Combining near-infrared illuminants to optimize venous imaging*. Medical Imaging. Vol. 6509. 2007: SPIE.
61. Paquit, V.C., et al. *Simulation of skin reflectance images using 3D tissue modeling and multispectral Monte Carlo light propagation*. in *2008 30th Annual International Conference of the IEEE Engineering in Medicine and Biology Society*. 2008.
62. Ayers, F., et al., *Fabrication and characterization of silicone-based tissue phantoms with tunable optical properties in the visible and near infrared domain*. SPIE BiOS. Vol. 6870. 2008: SPIE.
63. Firbank, M., M. Oda, and D.T. Delpy, *An improved design for a stable and reproducible phantom material for use in near-infrared spectroscopy and imaging.* Phys Med Biol, 1995. **40**(5): p. 955-61.
64. Hayakawa, C.K., et al., *Optical sampling depth in the spatial frequency domain.* J Biomed Opt, 2019. **24**(7).

65. Mourant, J.R., et al., *Mechanisms of light scattering from biological cells relevant to noninvasive optical-tissue diagnostics.* Appl Opt, 1998. **37**(16): p. 3586-93.

Papers

The papers associated with this thesis have been removed for copyright reasons. For more details about these see:

https://doi.org/10.3384/9789180751155

FACULTY OF SCIENCE AND ENGINEERING

Linköping studies in science and technology. Licentiate Thesis Nr. 1956, 2023
Department of Biomedical Engineering

Linköping University
SE-581 83 Linköping, Sweden

www.liu.se